MELTING LAYER ANALYSIS OF IN-SITU OBSERVATIONS OBTAINED FROM MULTIPLE FIELD PROJECTS

Logan Twohey

Master's Thesis Defense

University of North Dakota

July 15th, 2022

Committee Chair:

Dr. David Delene, UND

Committee Members:

Dr. Michael Poellot, UND

Dr. Andrew Heymsfield, NCAR

Motivation

- The melting layer is the transition from ice to liquid in cold precipitating cloud systems.
- Most studies on the melting layer have been through remote sensing with radar, laboratory experiments, and numerical models.
- Relatively few studies have used in-situ observations due to difficulties in direct measurements.
- In-situ observations can improve the representation of melting layer microphysics.

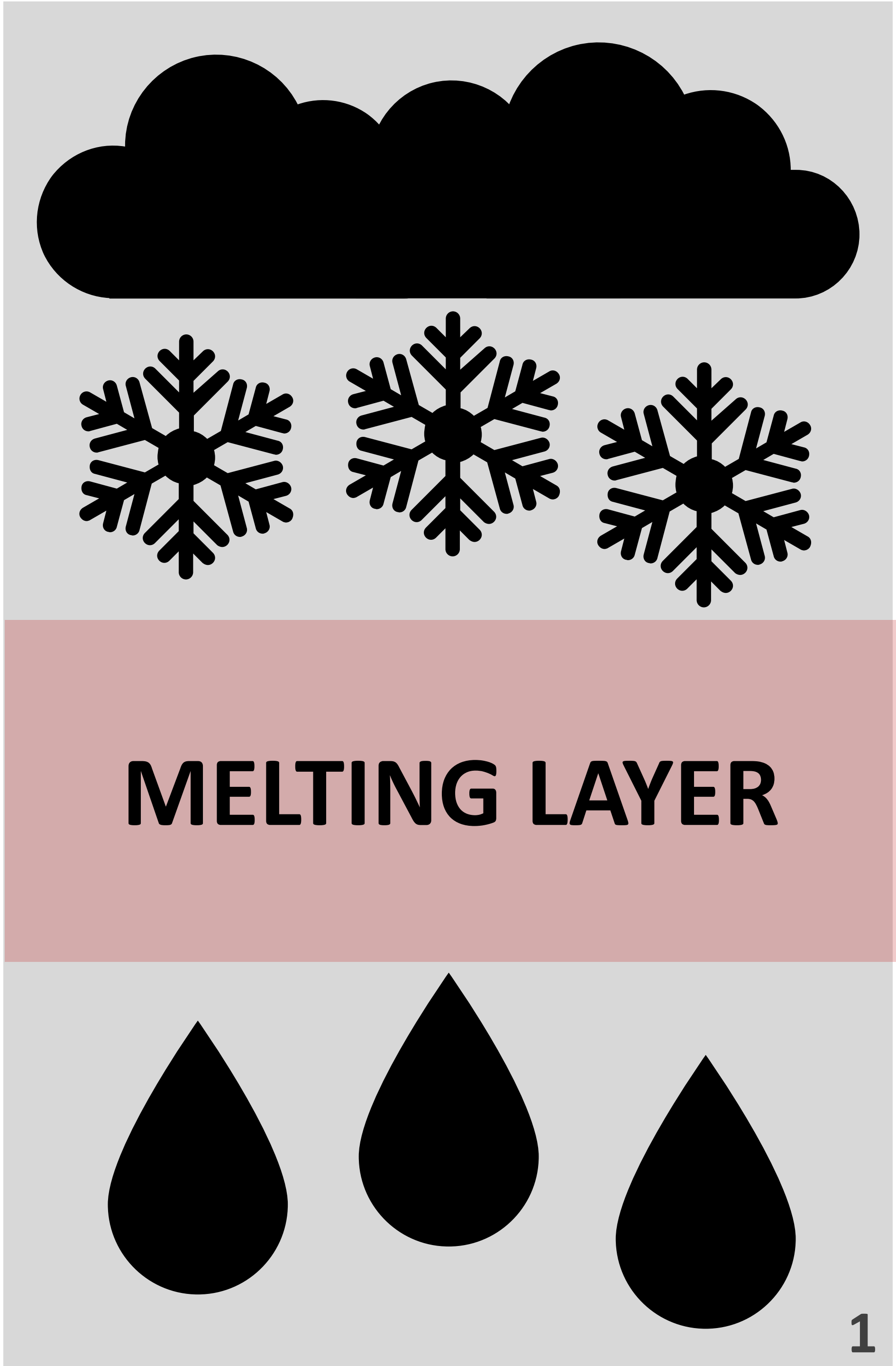

Radar Bright Band Signal

- Magnitude up to 10 dBZ.
- **Contributing Factors**
  - Increase in dielectric constant of hydrometeors beginning to melt
  - Nonsphericity of melting hydrometeors
  - Enhanced aggregation
  - Coupling of aggregation and breakup

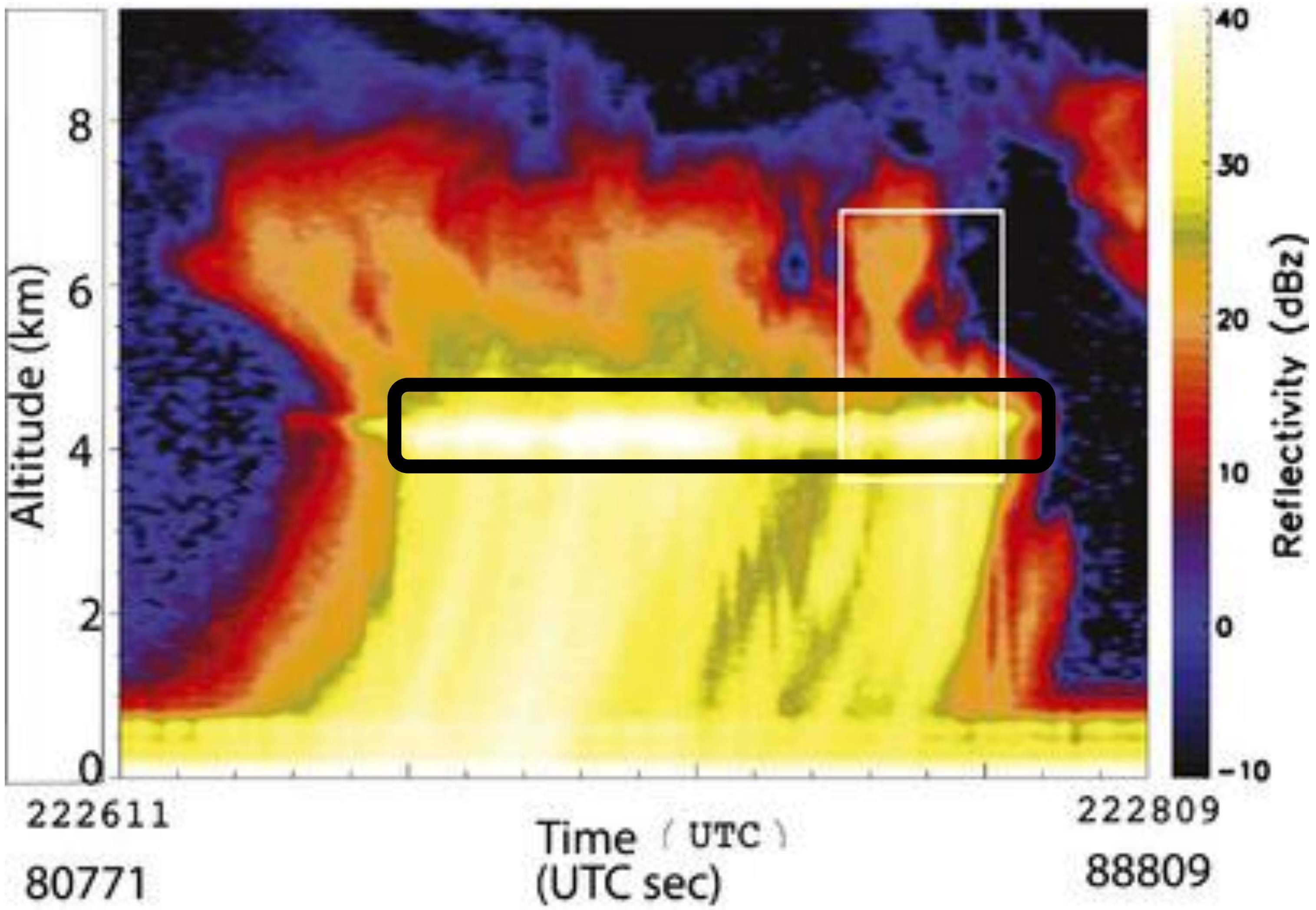

Adapted from Heymsfield et al. (2015) Figure 2

(Quasi)-isothermal Layer

- Diabatic cooling due to melting associated with a 0 °C isothermal or quasi-isothermal layer:
  - Deepens the melting layer
  - Produces mesoscale circulations
  - Enhances frontogenesis
  - Processes are important in forecasting surface precipitation type

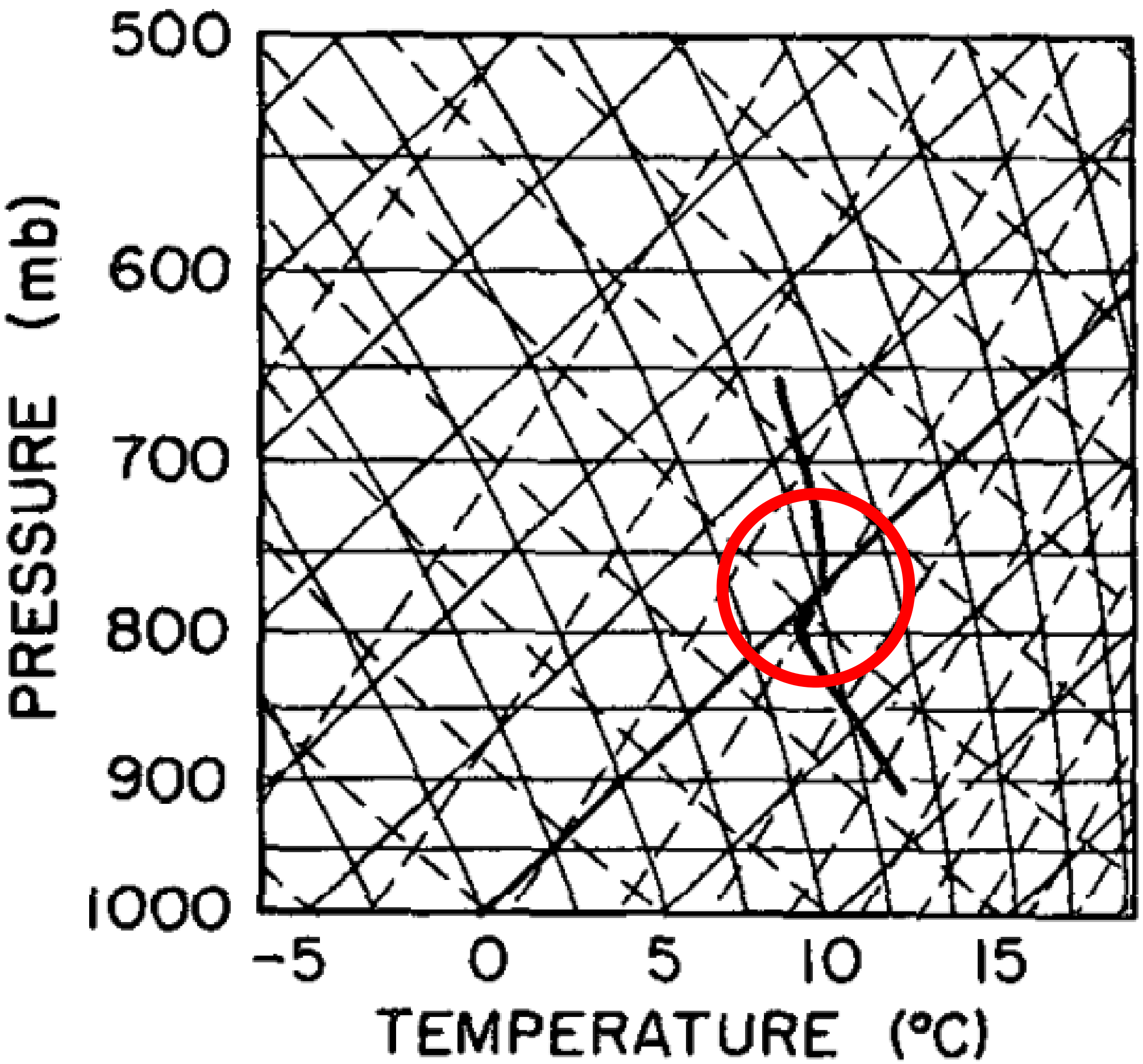

Adapted from Stewart et al. (1984) Figure 12

Summary of Findings From In-situ Studies

- Large aggregates are the most common hydrometeor at 0 °C.
- Aggregation is enhanced within the melting layer.

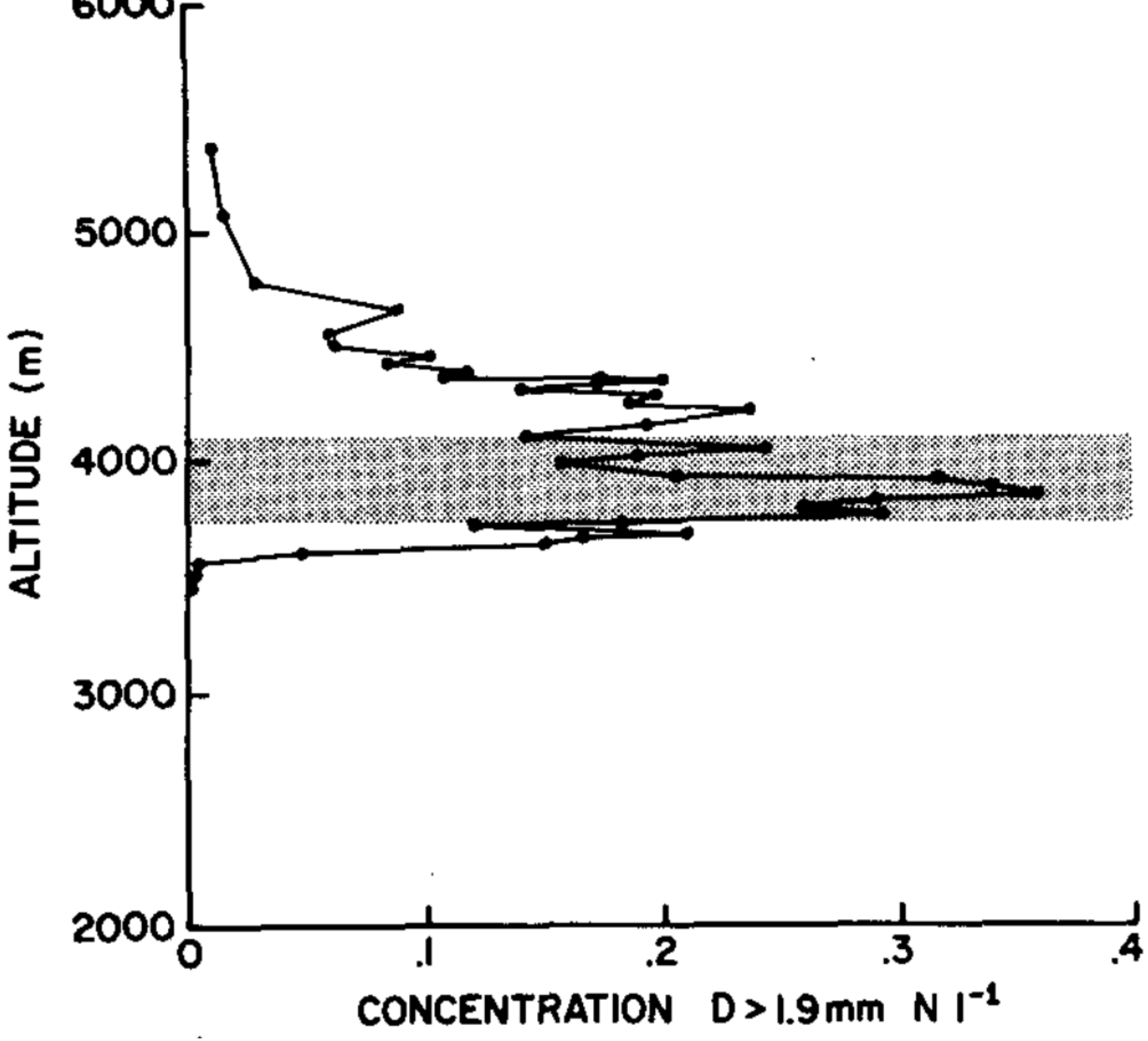

Adapted from Willis and Heymsfield (1989) Figure 9

Summary of Findings From In-situ Studies

- Large aggregates are the most common hydrometeor at 0 °C.
- Aggregation is enhanced within the melting layer.
- Relative humidity influences the melting process.

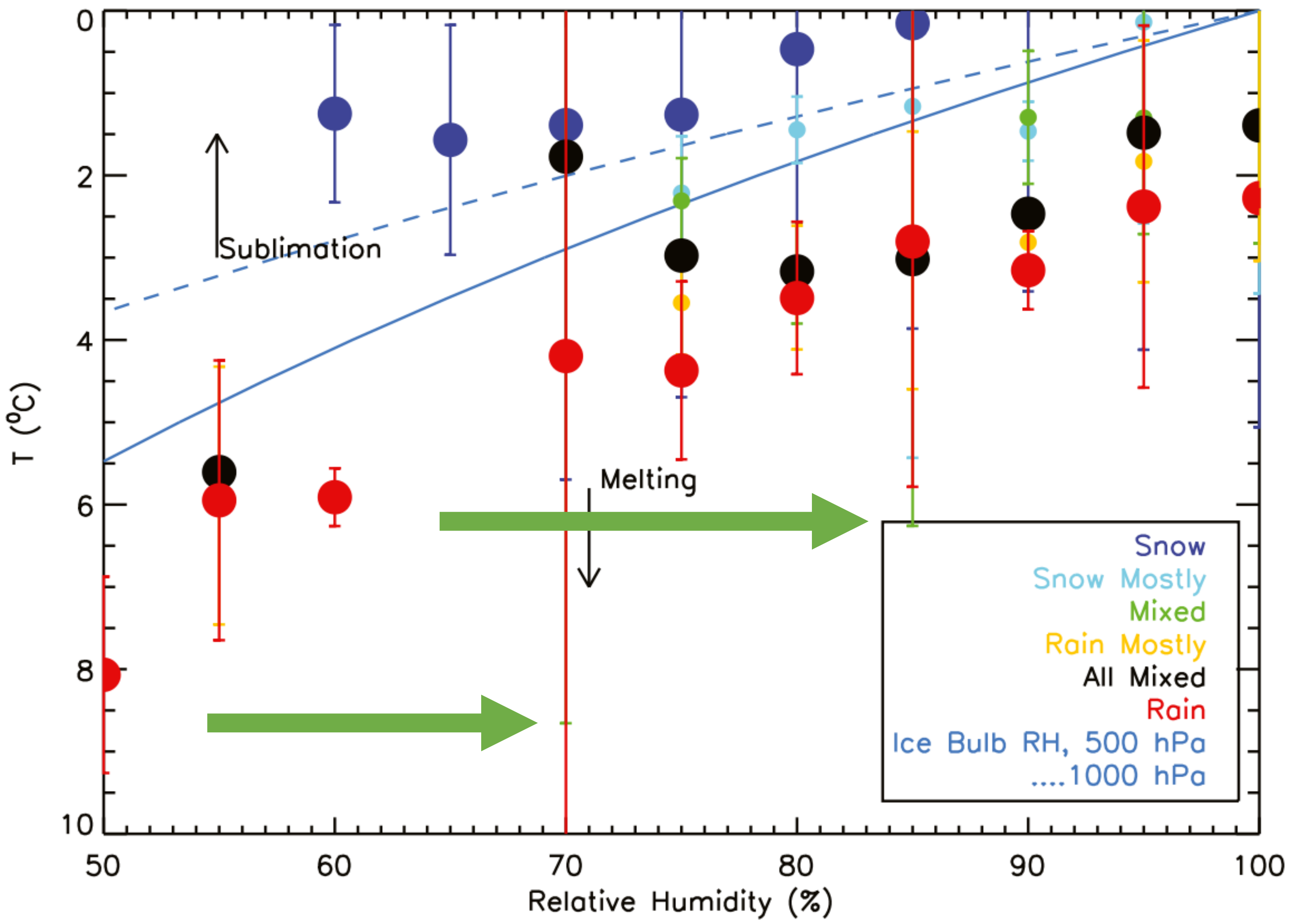

Adapted from Heysmfield et al. (2021) Figure 12

Summary of Findings From In-situ Studies

- Large aggregates are the most common hydrometeor at 0 °C.
- Aggregation is enhanced within the melting layer.
- Relative humidity influences the melting process.
- Melting causes an increase in hydrometeor area ratio.

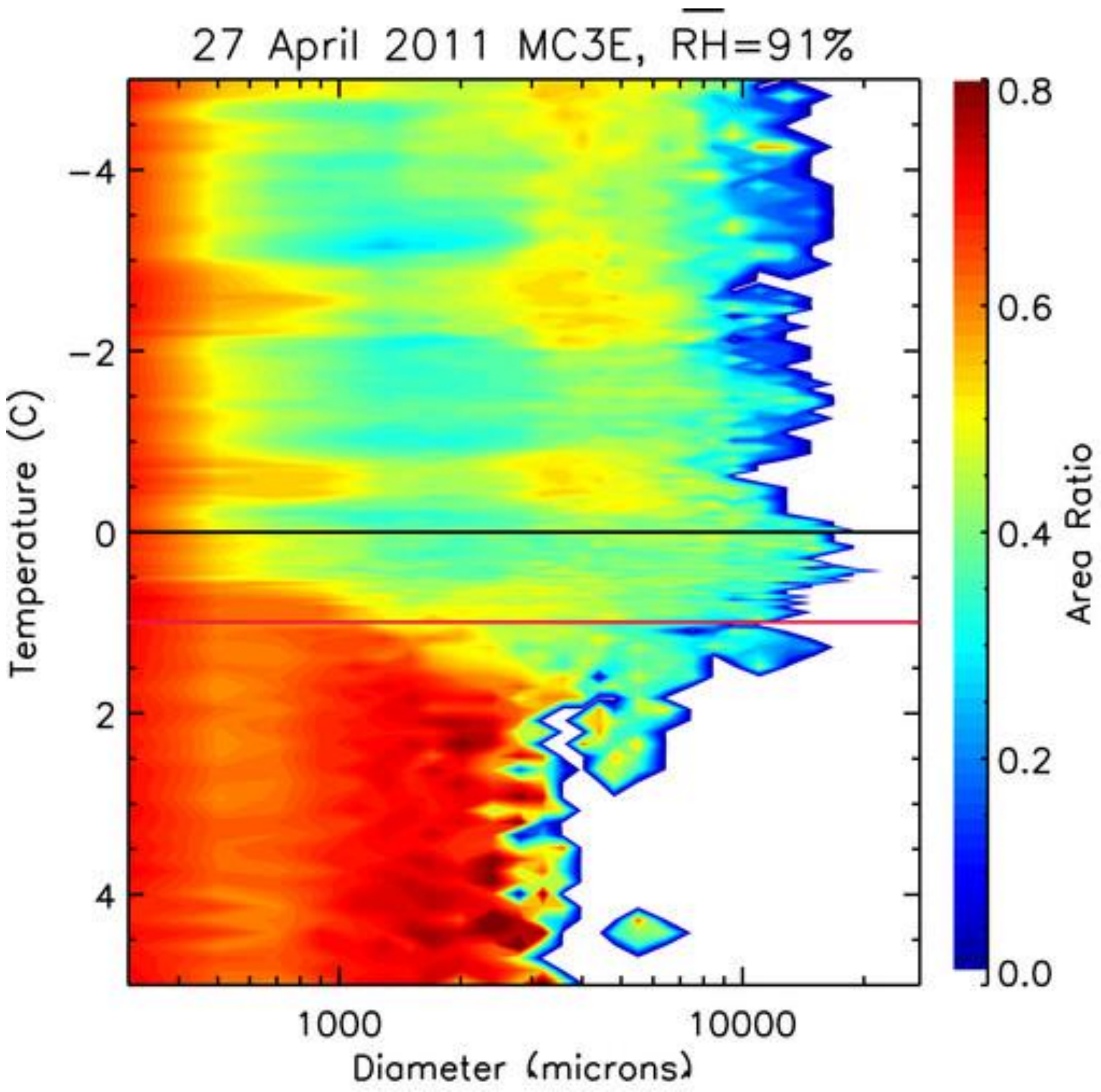

Adapted from Heymsfield et al. (2015) Figure 19

Summary of Findings From In-situ Studies

- Large aggregates are the most common hydrometeor at 0 °C.
- Aggregation is enhanced within the melting layer.
- Relative humidity influences the melting process.
- Melting causes an increase in hydrometeor area ratio.
- Melting modifies the particle size distribution.

$$N(D) = N_0 e^{-\lambda D}$$

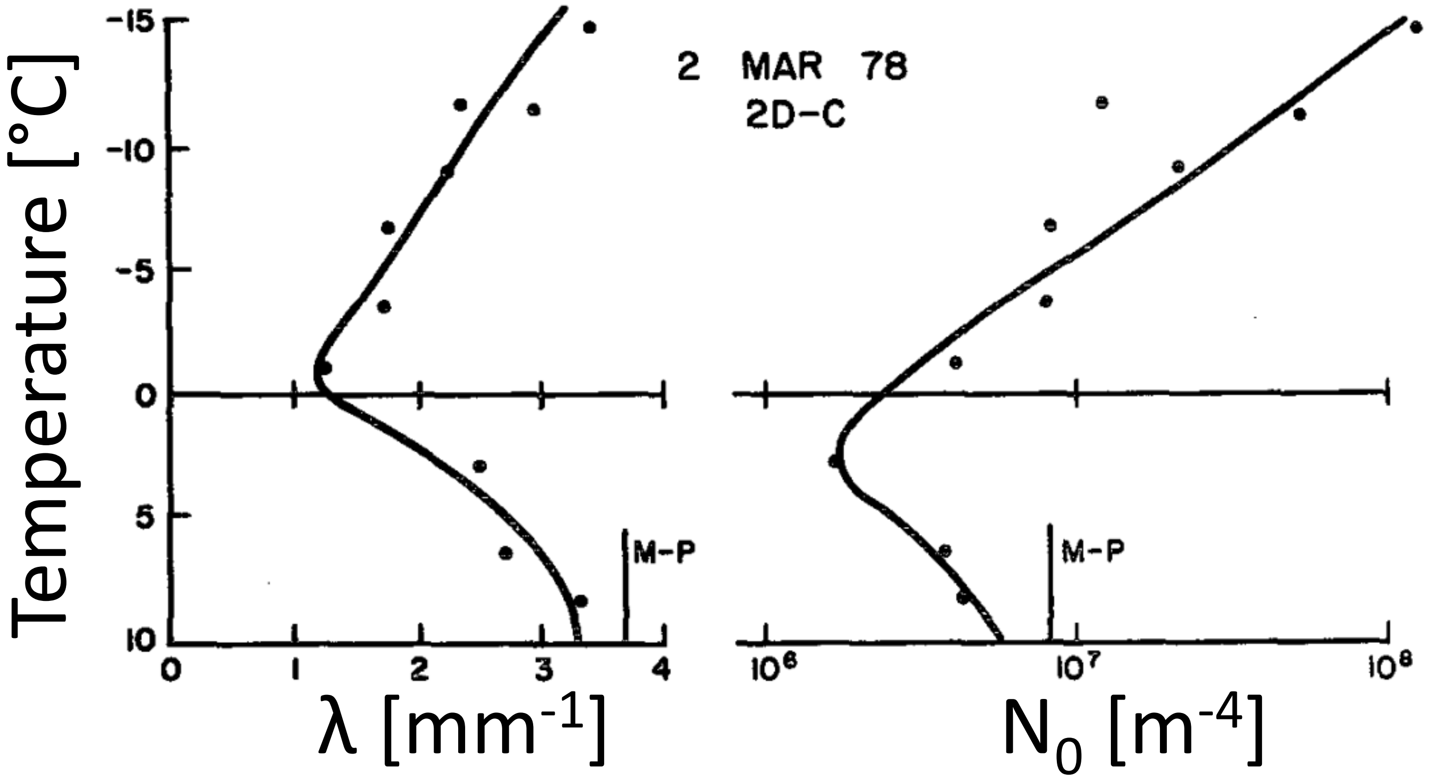

Adapted from Stewart et al. (1984) Figure 9

Objective

- Extend previous in-situ analysis of the melting layer:
  - Characterize the particle size distribution and area ratio.
  - Determine the impact of relative humidity on the melting process.

- Use direct observations from several recent NASA field campaigns which includes a variety of environments and storm types.

NASA Field Campaigns

Project	Year	Season	Location	Cloud	Precipitation
MC3E	2011	Spring	Great Plains	2D-C	HVPS3
GCPEX	2012	Winter	Georgian Bay	2D-C	HVPS3
IPHEX	2014	Spring	Southeast US	2D-S	HVPS3
OLYMPEX	2015*	Late Fall	Western Washington	2D-S	(2) HVPS3
IMPACTS	2020	Winter	Northeast US	2D-S	(2) HVPS3

Imaging Probes

- **Two-Dimensional Stereo (2D-S)** probe has 10 µm pixel resolution
- **High Volume Precipitation Spectrometer Version 3 (HVPS3)** has 150 µm pixel resolution
- Data processed with the **ADPAA** software package and utilizes the **SODA2**

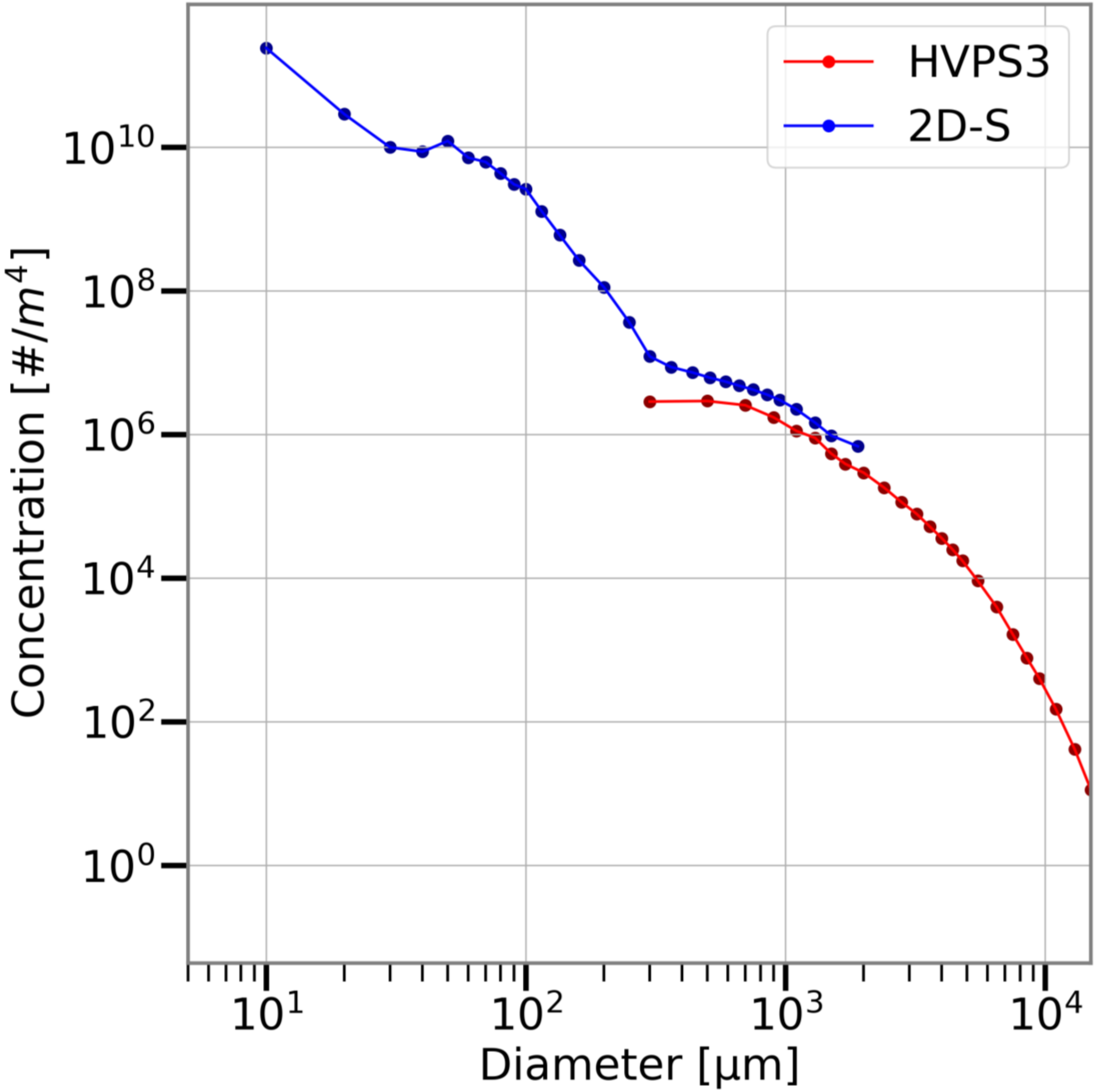

Imaging Probes

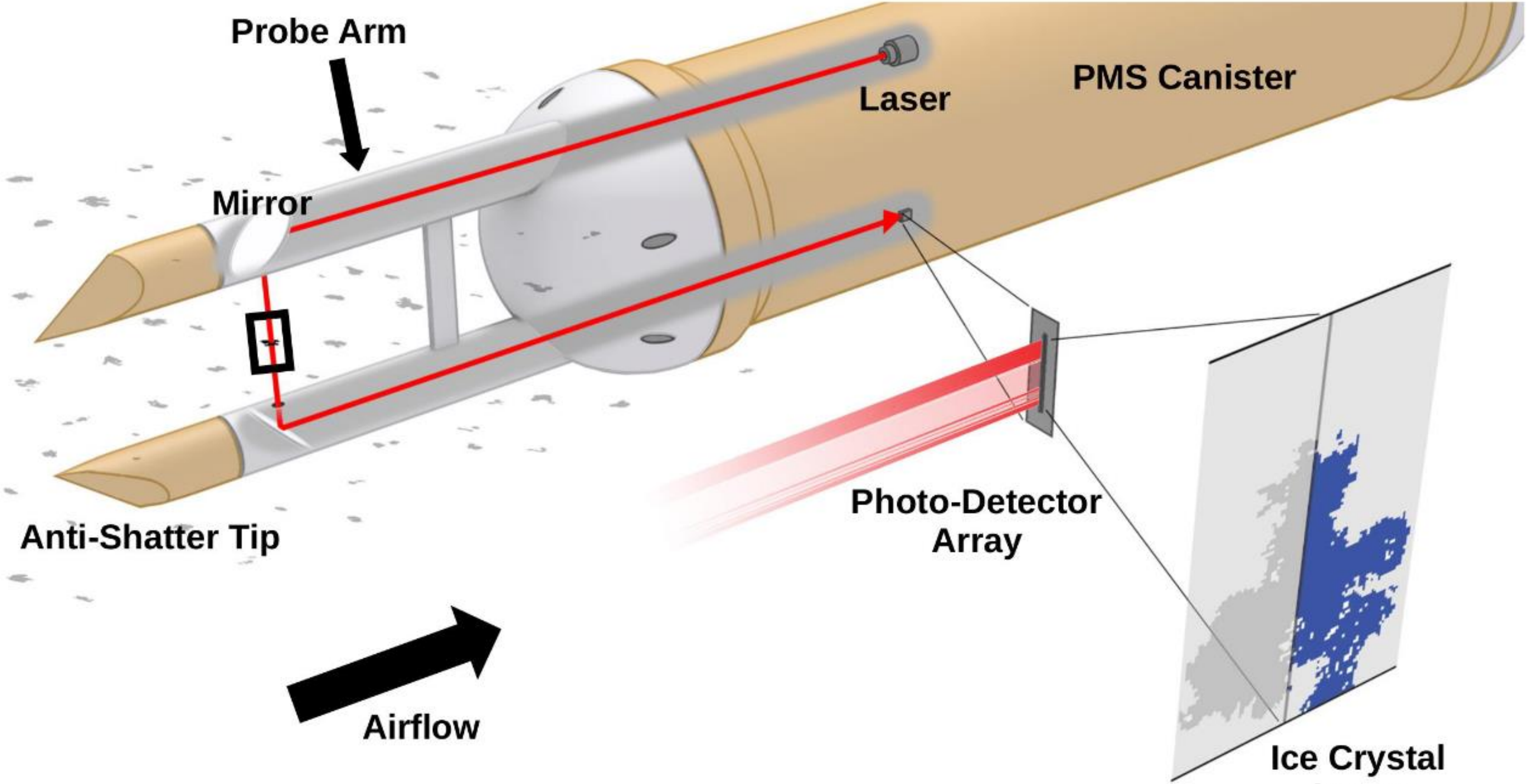

Adapted from Wagner and Delene (2022) Figure 1

Area Ratio

	2D-S	HVPS3
Image Size [μm^2]	282,400	270,000
Fast Circle [μm^2]	303,054	368,212
Area Ratio	**0.93**	**0.73**

- **Area ratio** is the ratio of the particle image area to the fast circle area.
- Low resolution probes such as the HVPS3 have lower area ratio for circular hydrometeors.

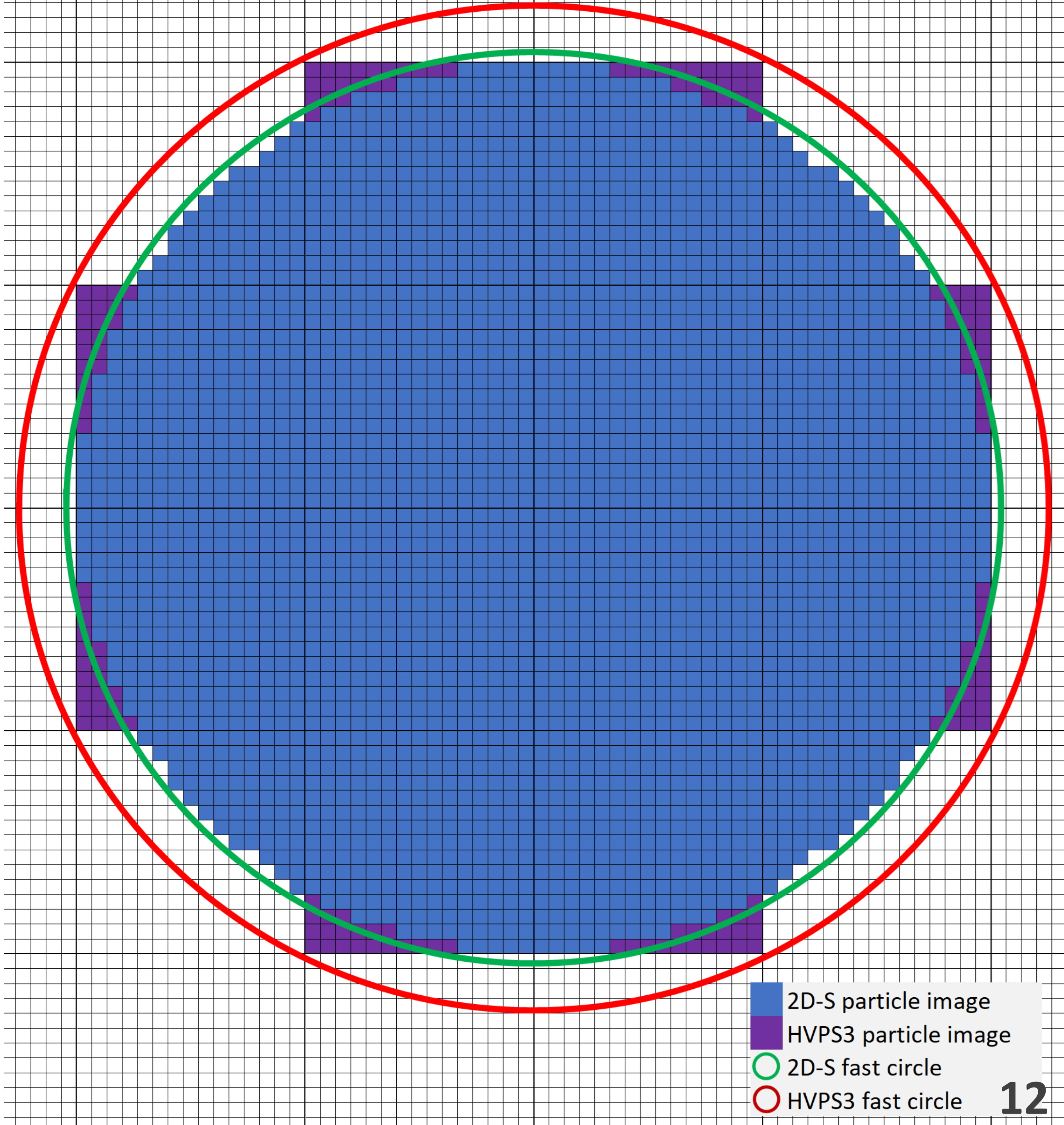

Melting Layer Depth

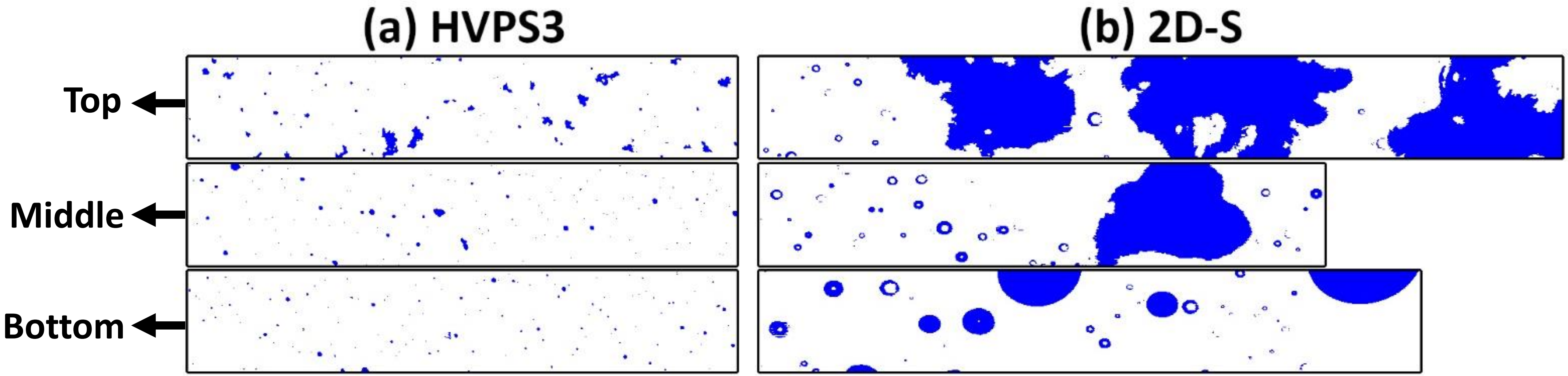

- **Top:** 0 °C ice-bulb isotherm (frozen hydrometeors, typically aggregates)
- **Middle:** Mixed phase & partially melted hydrometeors
- **Bottom:** All hydrometeors melted – images appear fully round

Ice-bulb Temperature Calculation

- **Ice-bulb temperature** (and wet-bulb) calculated with the new *bulbtemp* ADPAA module that inputs:
  - Air temperature
  - Dew point temperature
  - Pressure

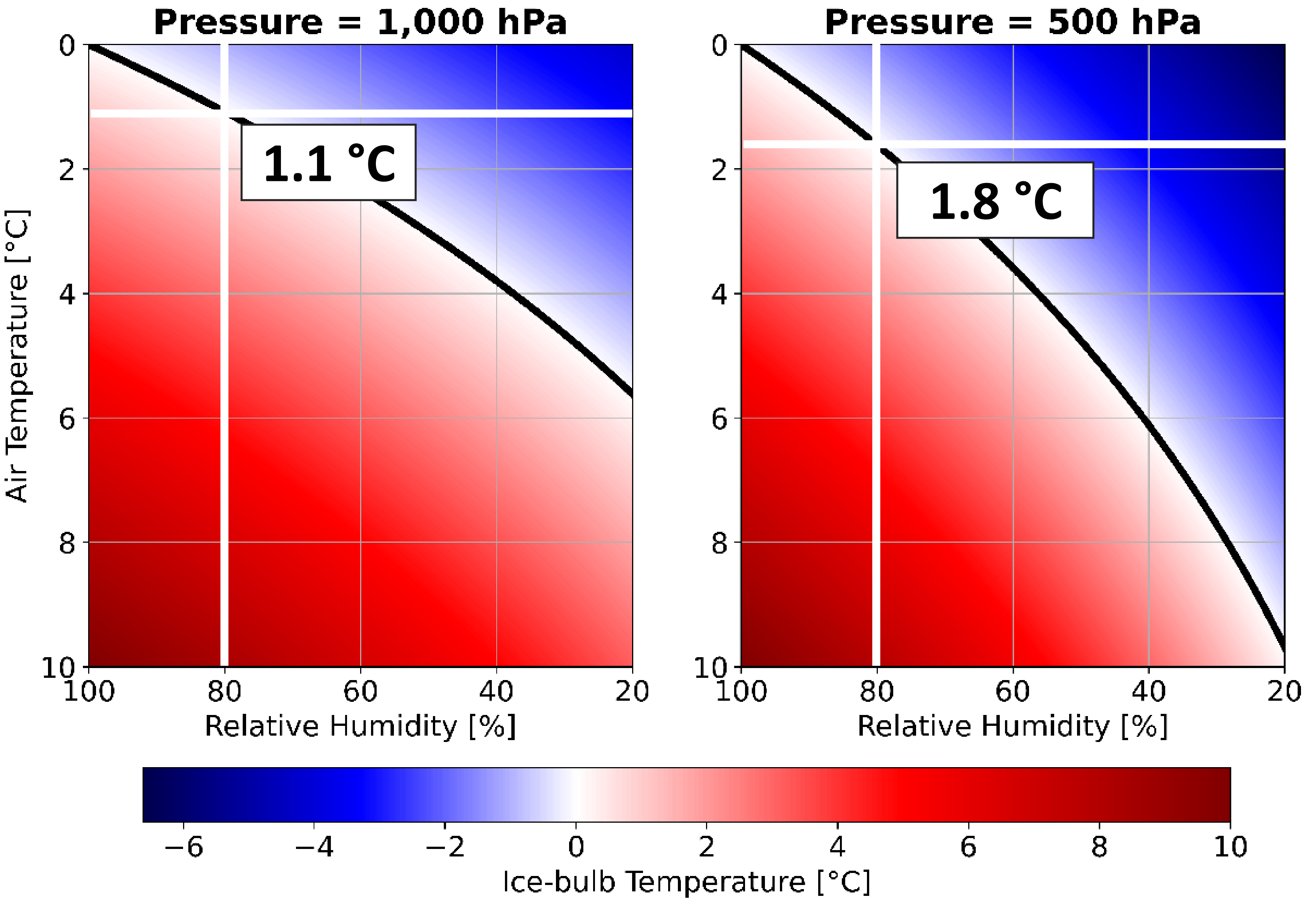

Melting Layer Profile

Melting Layer Criteria

- Continuous vertical measurements of hydrometeors melting
- Sampled during an ascent or descent
- Minimum hydrometeor concentration threshold of 10^3 #/m^4

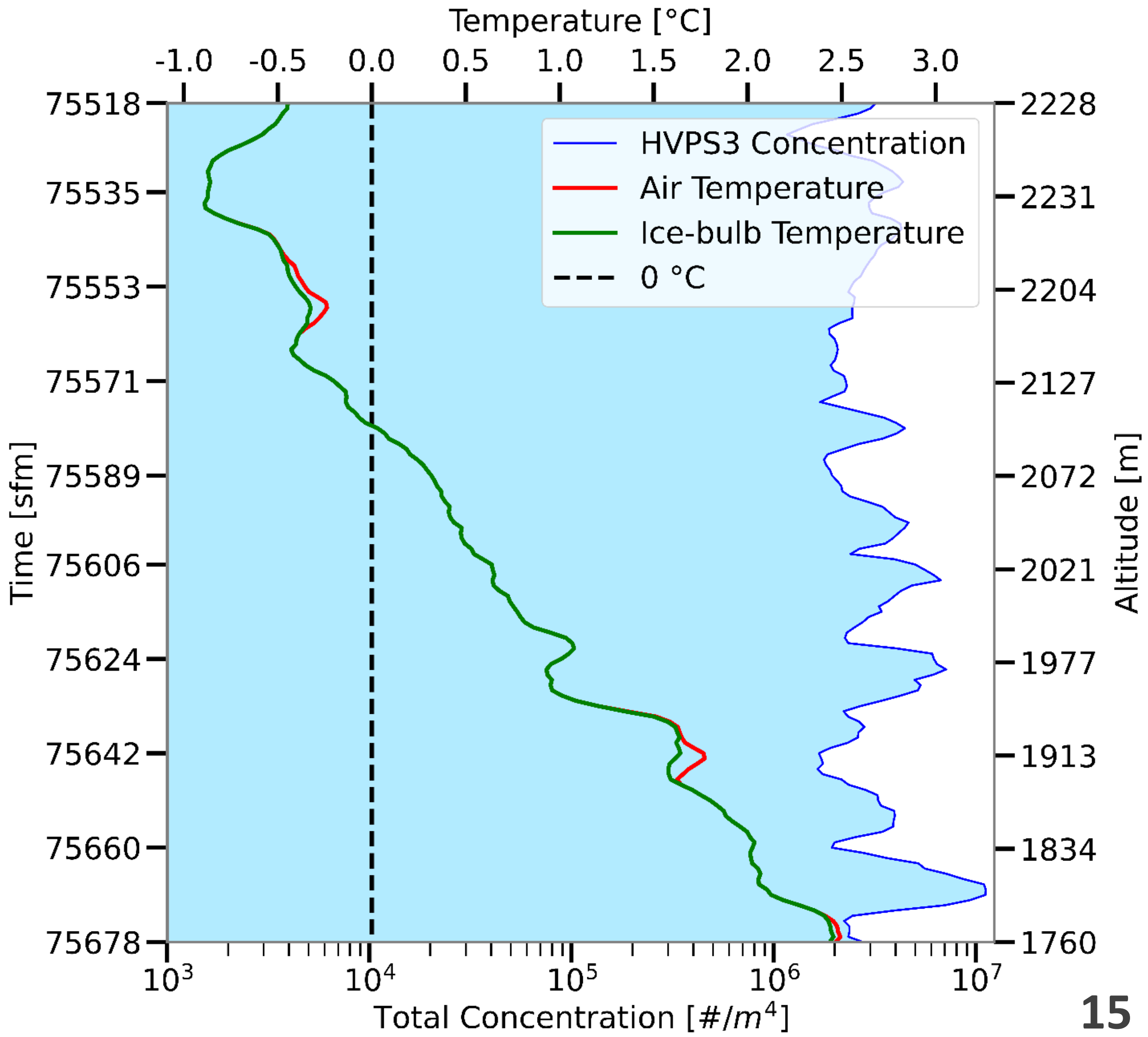

Penetration Type

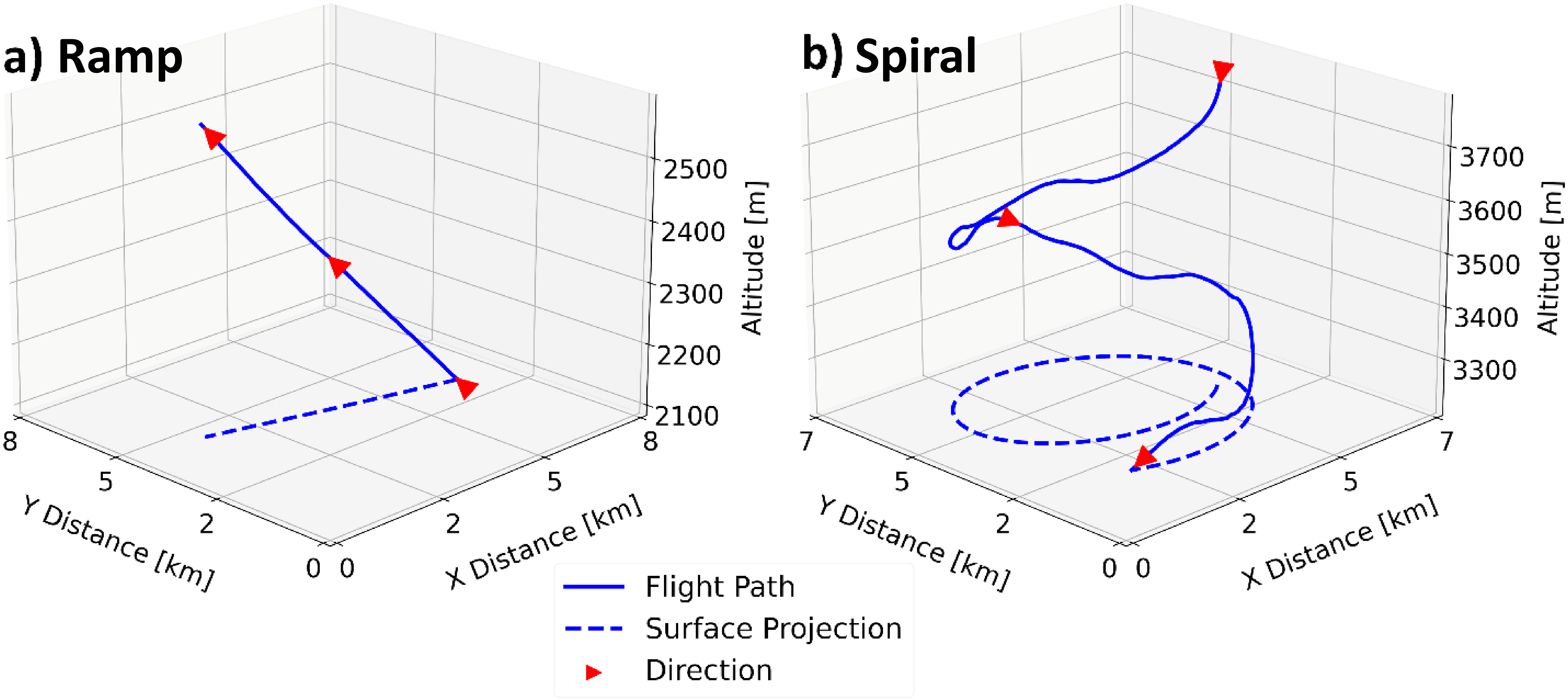

Melting Layer Cases

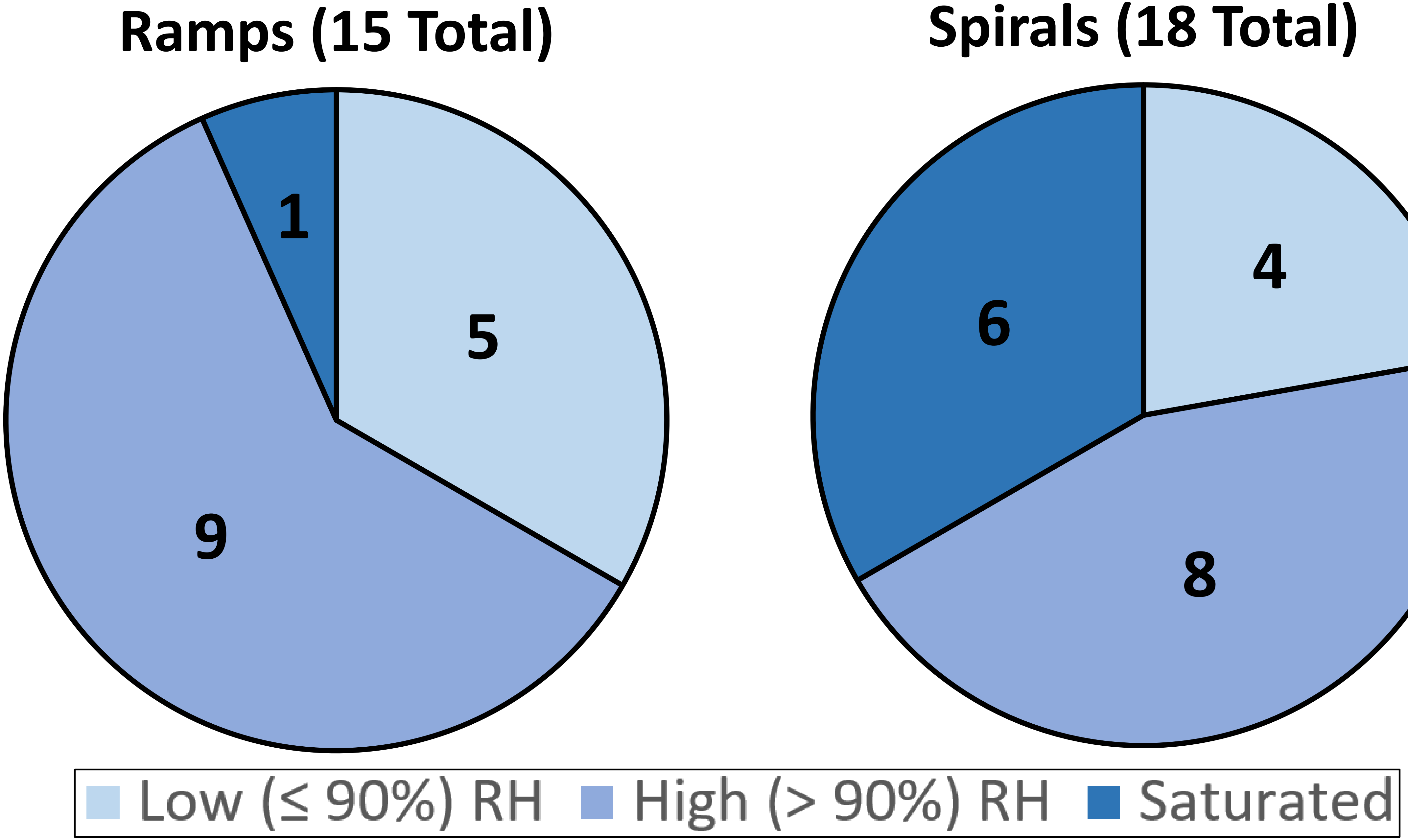

Melting Layer Cases

33 Total Cases → 5 Case Types

1. **High Relative Humidity -** OLYMPEX_Ram-Des_98RH
2. **Saturated -** OLYMPEX_Ram-Des_100RH
3. **Enhanced Aggregation**
   - IMPACTS_Spi-Des_94RH
   - MC3E_Ram-Asc_83RHa
4. **Low Relative Humidity** – GCPEX_Spi-Des_84RH
5. **Isothermal Layer** – GCPEX_Spi-Asc_100RH

High Relative Humidity

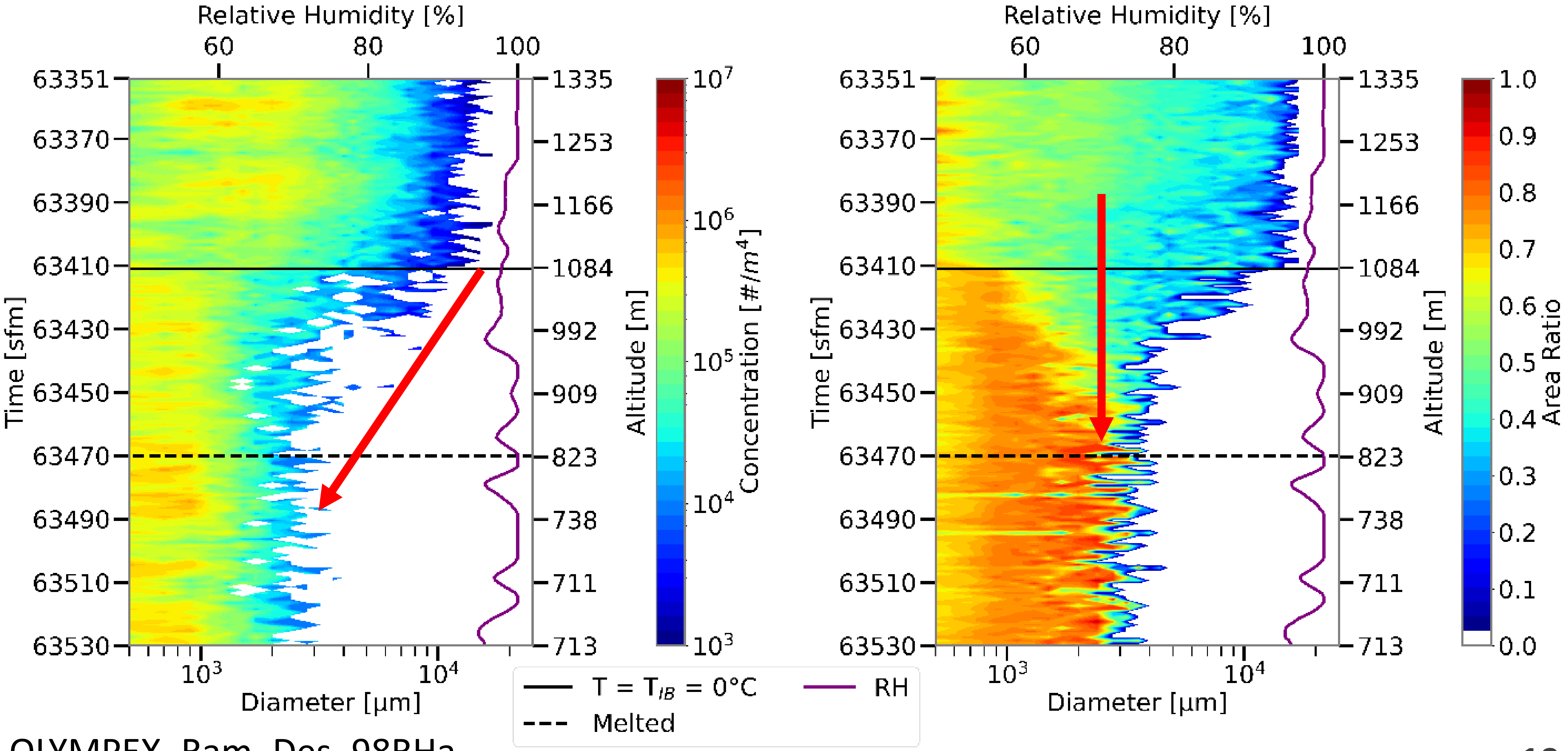

OLYMPEX_Ram_Des_98RHa

High Relative Humidity

- Both exponential fit parameters lowest above melting layer.
- Both increase as melting begins and concentration of large particles decreases.
- Most significant changes near the melting layer top.

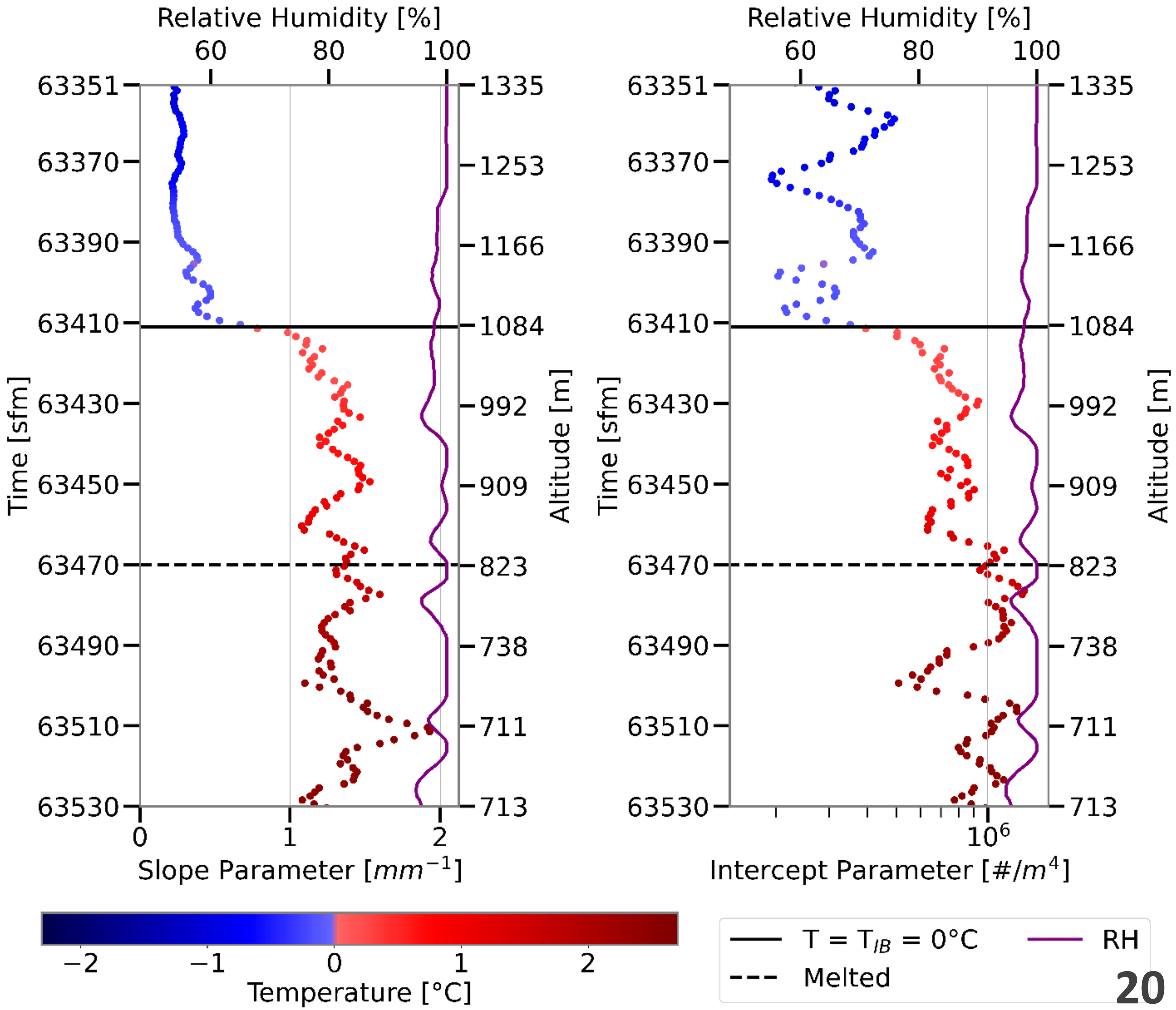

OLYMPEX_Ram_Des_98RHa

Saturated Case

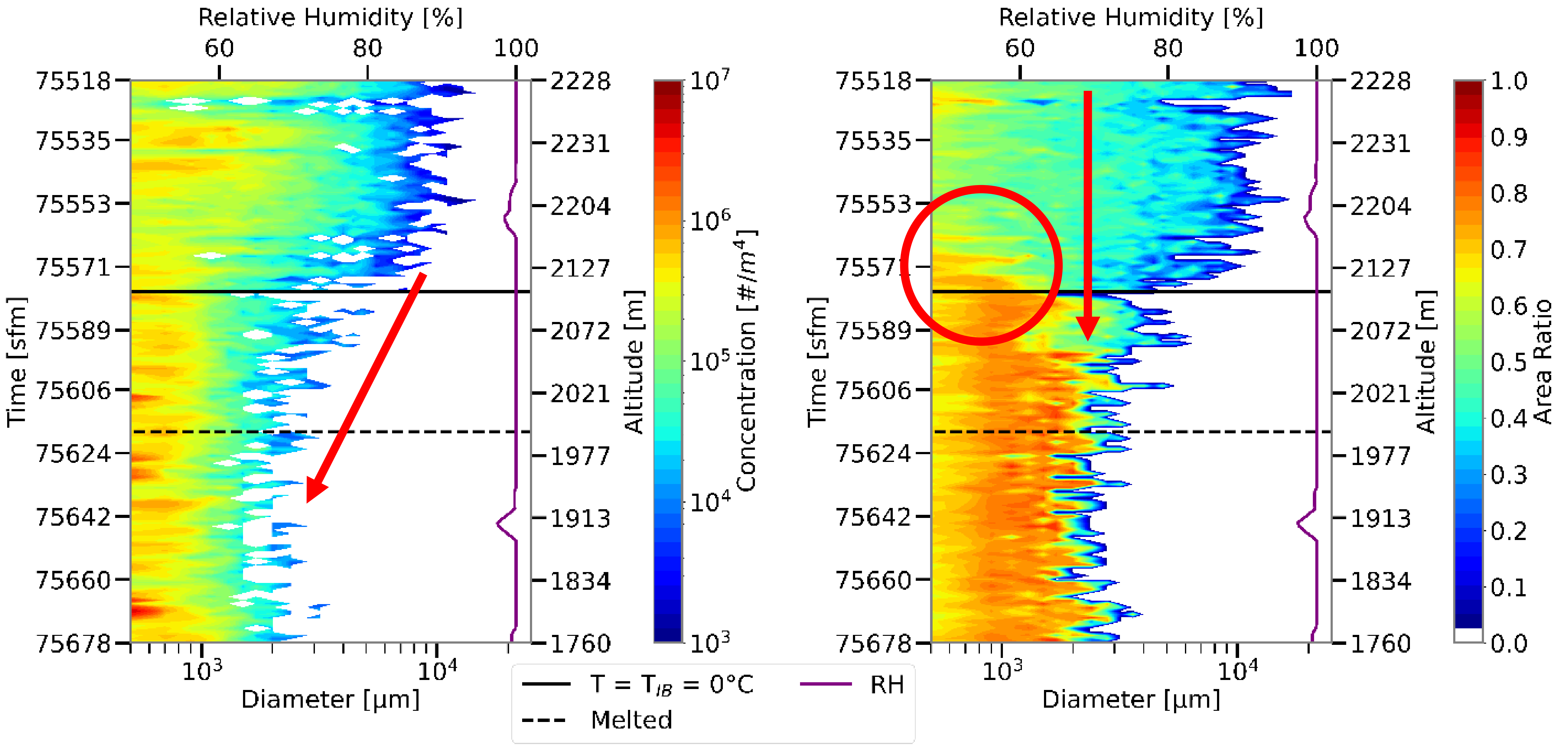

OLYMPEX_Ram_Des_100RH

Saturated Case

- Both parameters smallest above melting layer.
- Both parameters slightly larger below the melting layer than within.
- Distinct spikes in parameters associated with increases of small hydrometeor concentration.

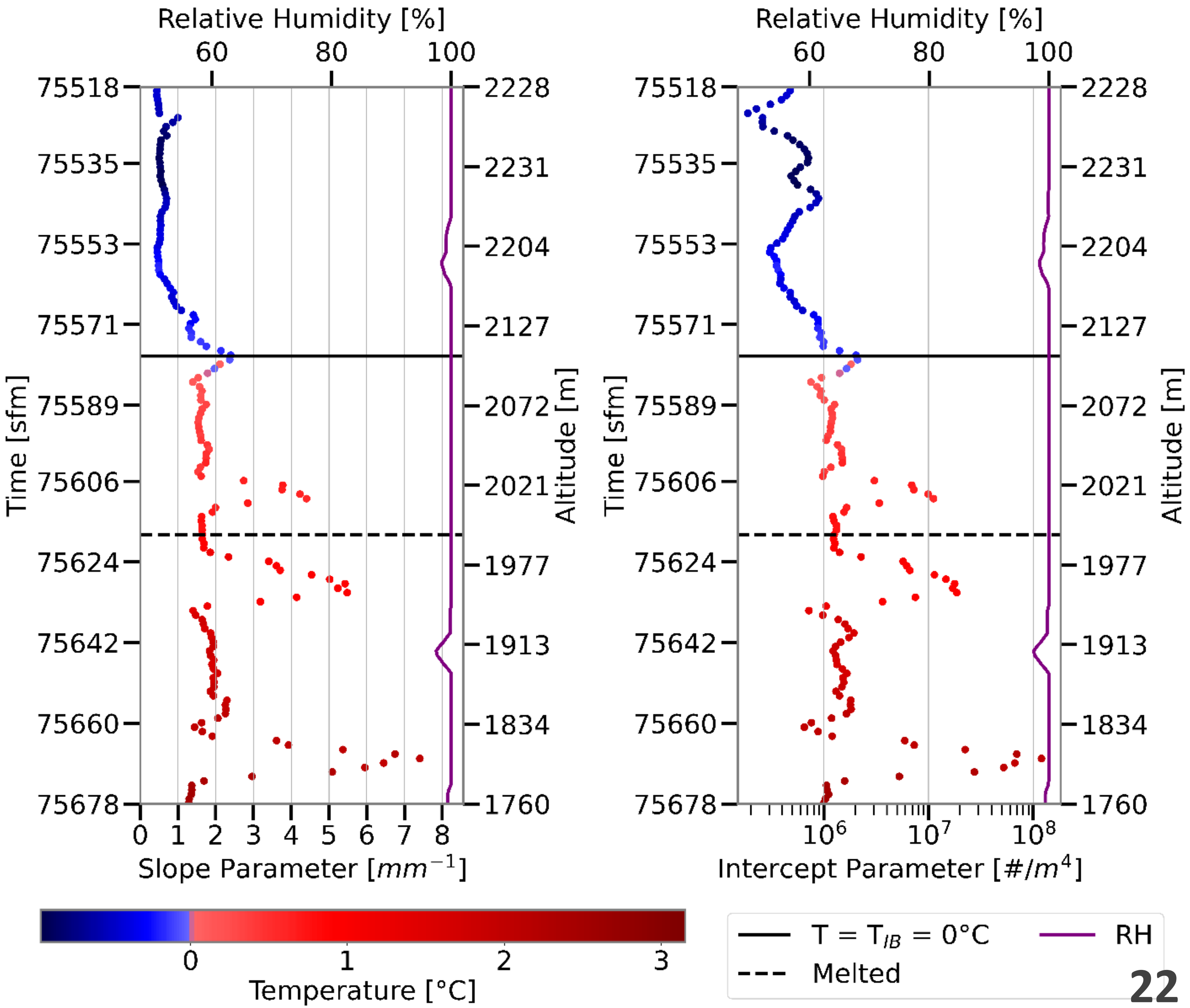

OLYMPEX_Ram_Des_100RH

Significant Aggregation Cases

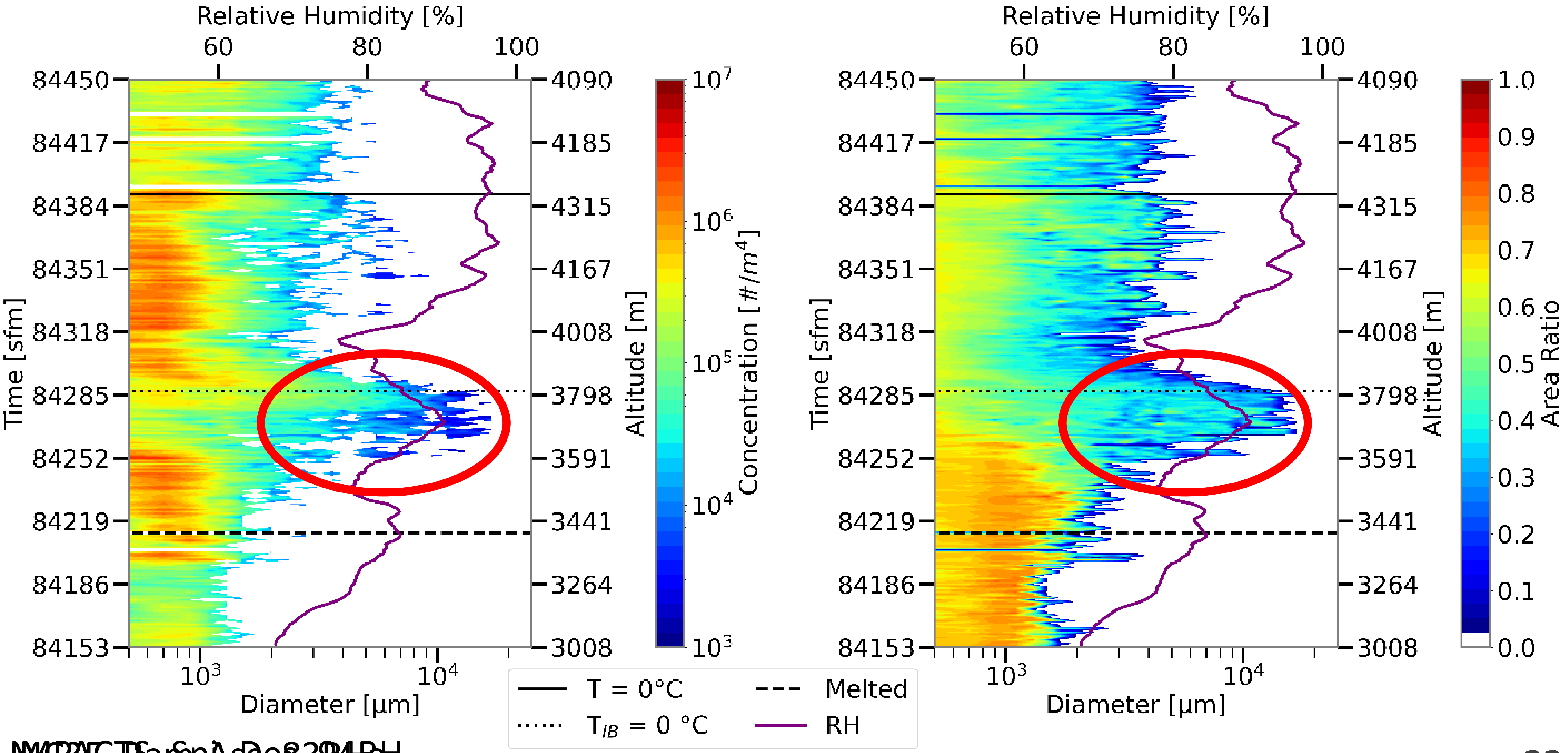

NCPAE_TS_anpi_Asd_e83 9RH

Low Relative Humidity

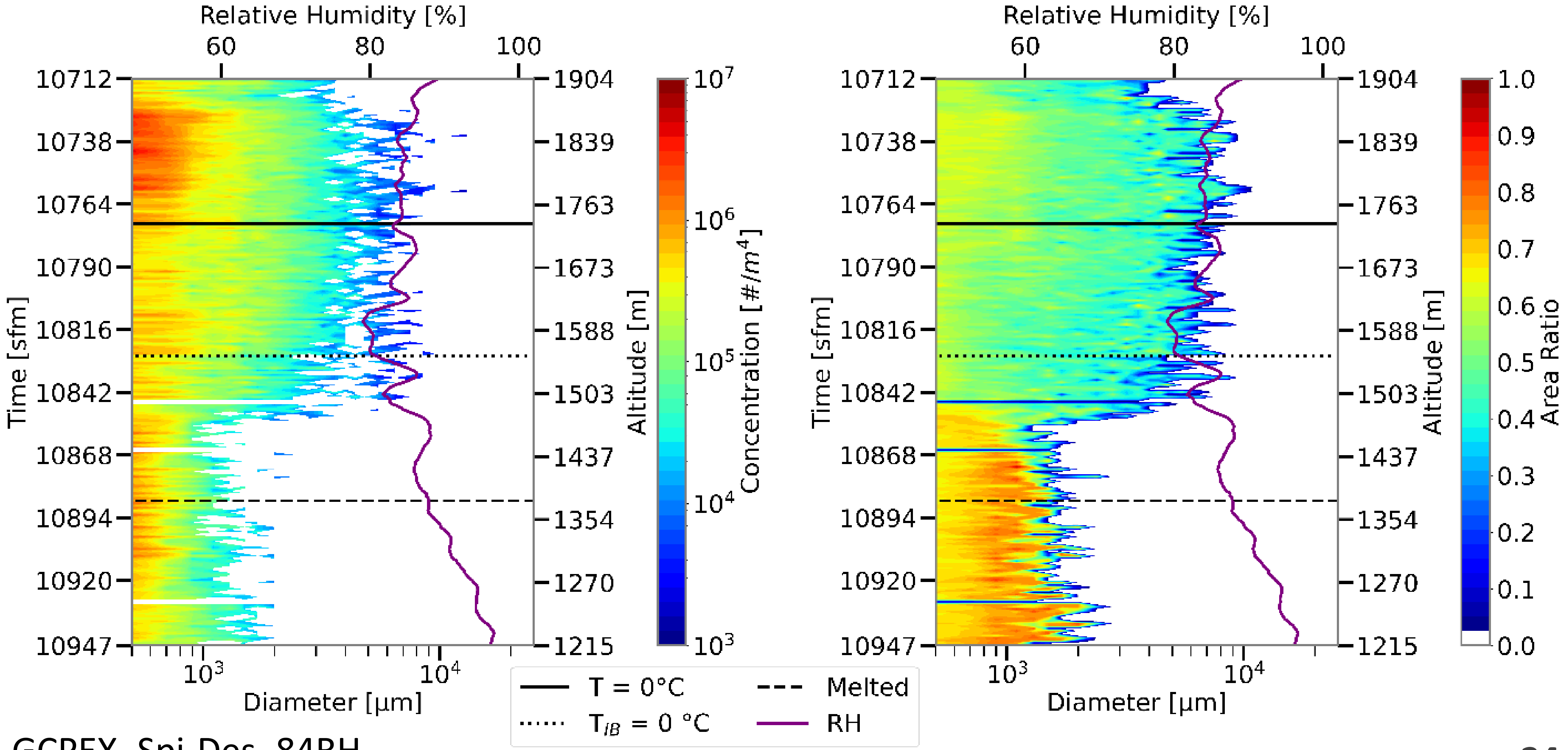

GCPEX_Spi-Des_84RH

Low Relative Humidity

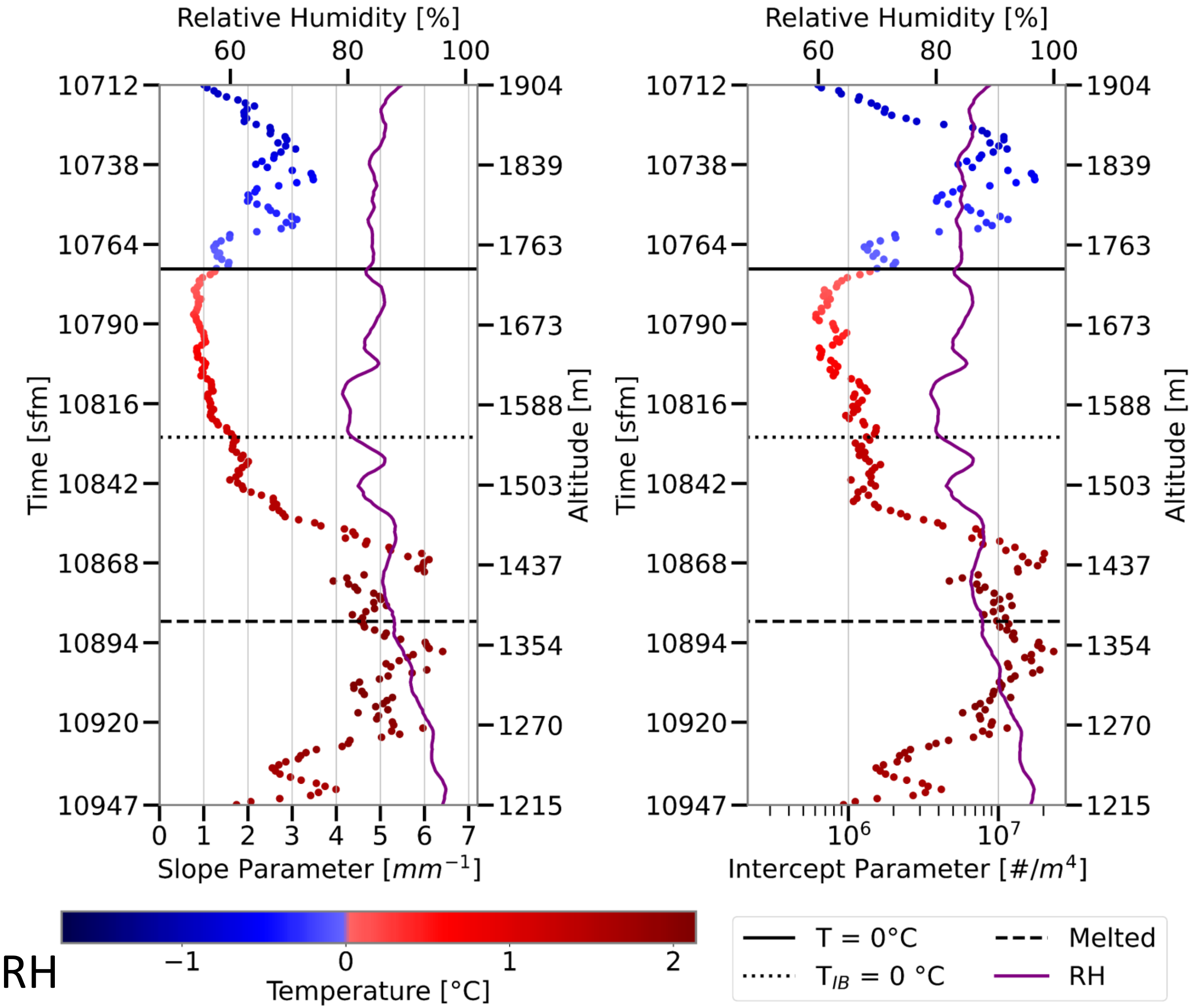

GCPEX_Spi-Des_84RH

Quasi-isothermal Layer

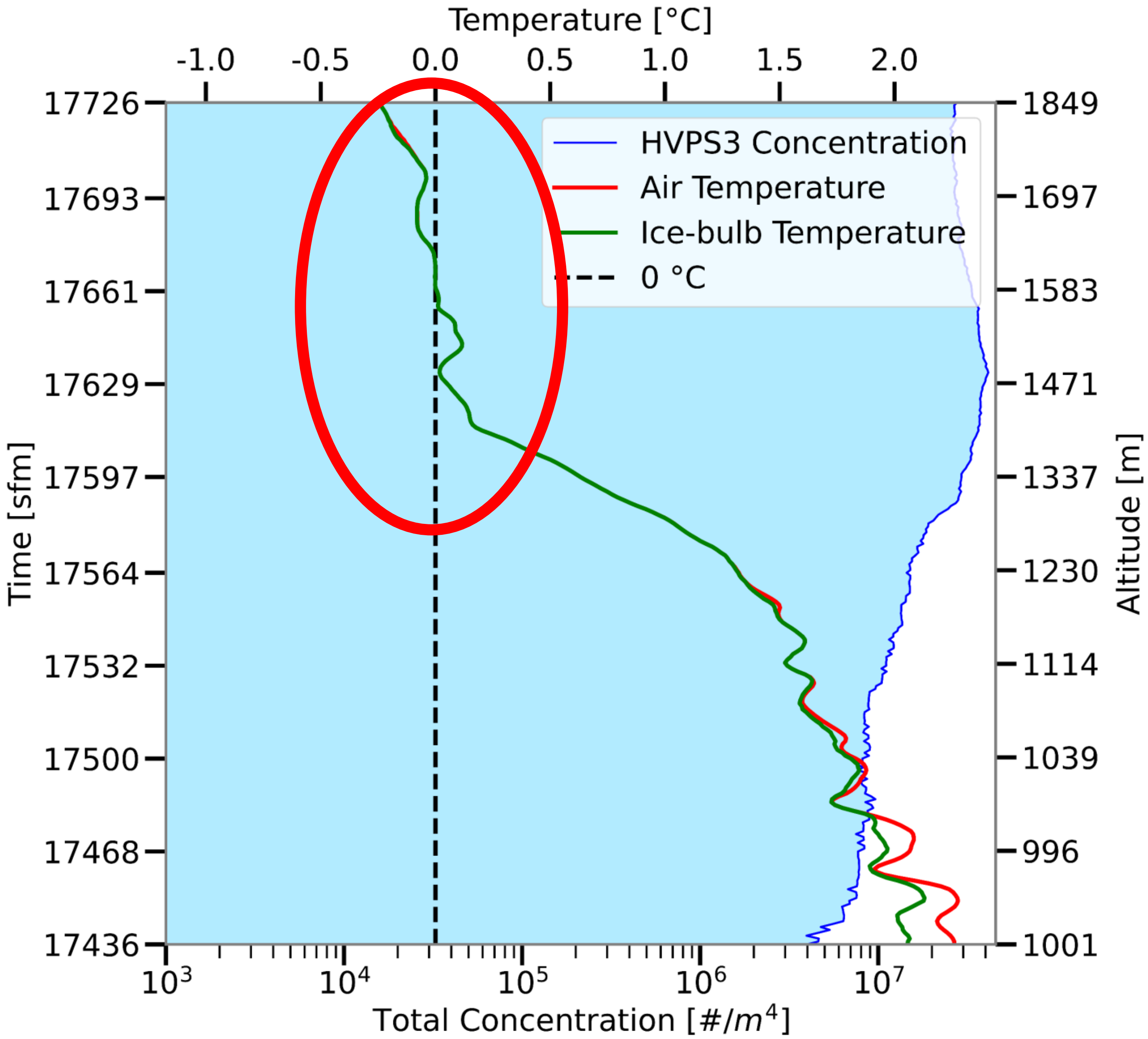

Results

- Concentration decreases
  - More frequent with low relative humidity
- Area ratio increases
- Max diameter decreases
- Exponential Fit
  - Slope parameter increases

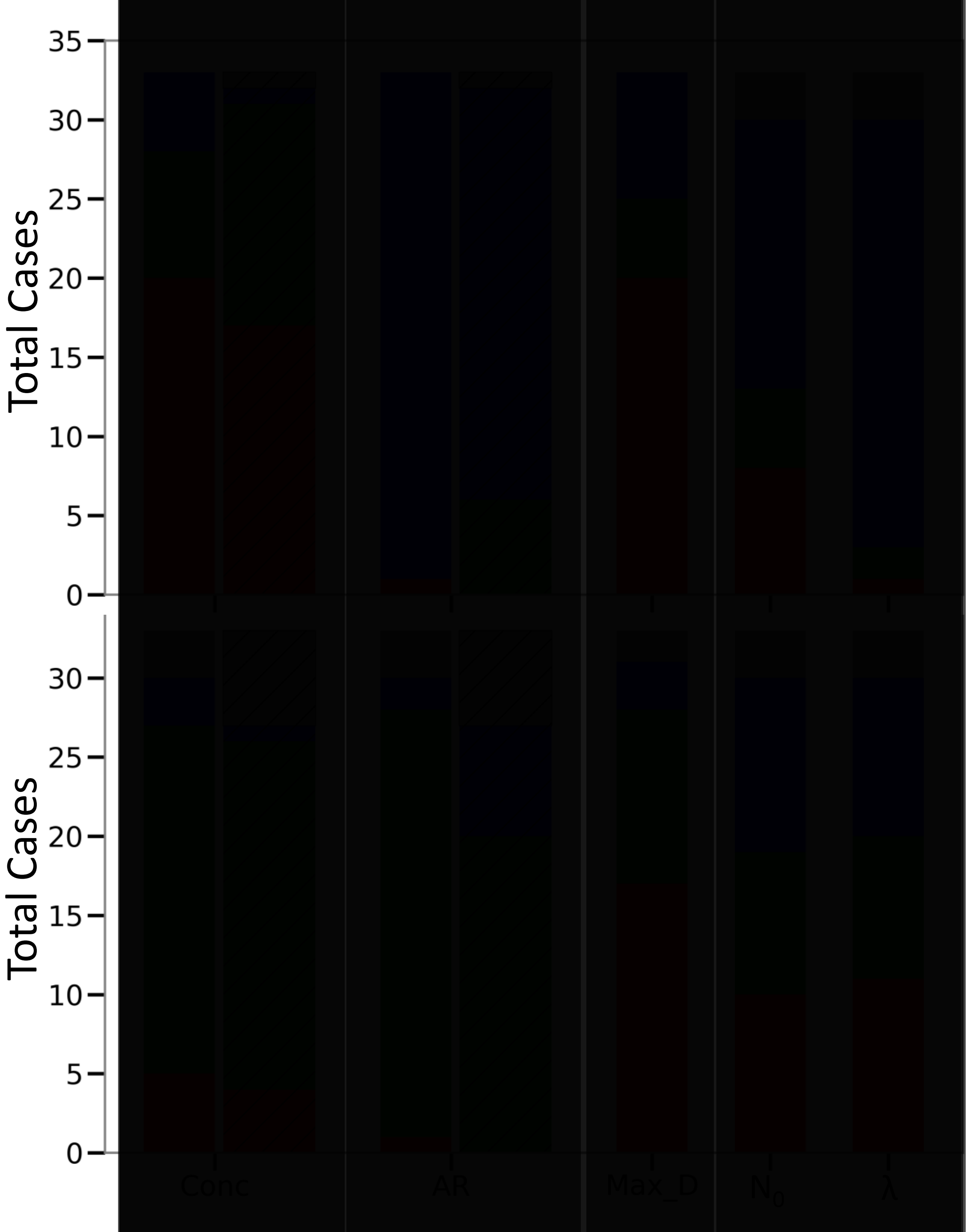

Above to Within Melting Layer

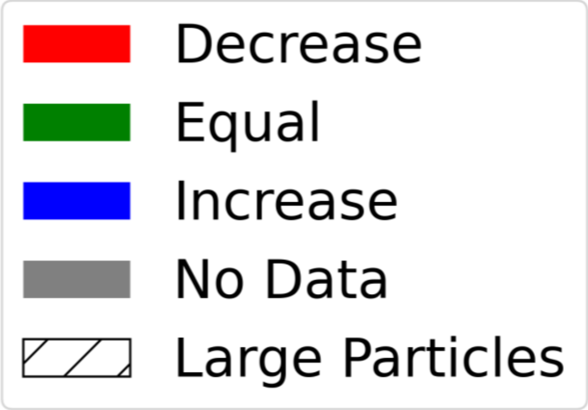

- **Conc** = Concentration
- **AR** = Area Ratio
- **Max_D** = Maximum Diameter
- $\mathbf{N_0}$ = Intercept Parameter
- **λ** = Slope Parameter

Within to Below Melting Layer

Results

- Concentration decreases
  - More frequent with low relative humidity
- Area ratio increases
- Max diameter decreases
- Exponential Fit
  - Slope parameter increases

Above to Within Melting Layer

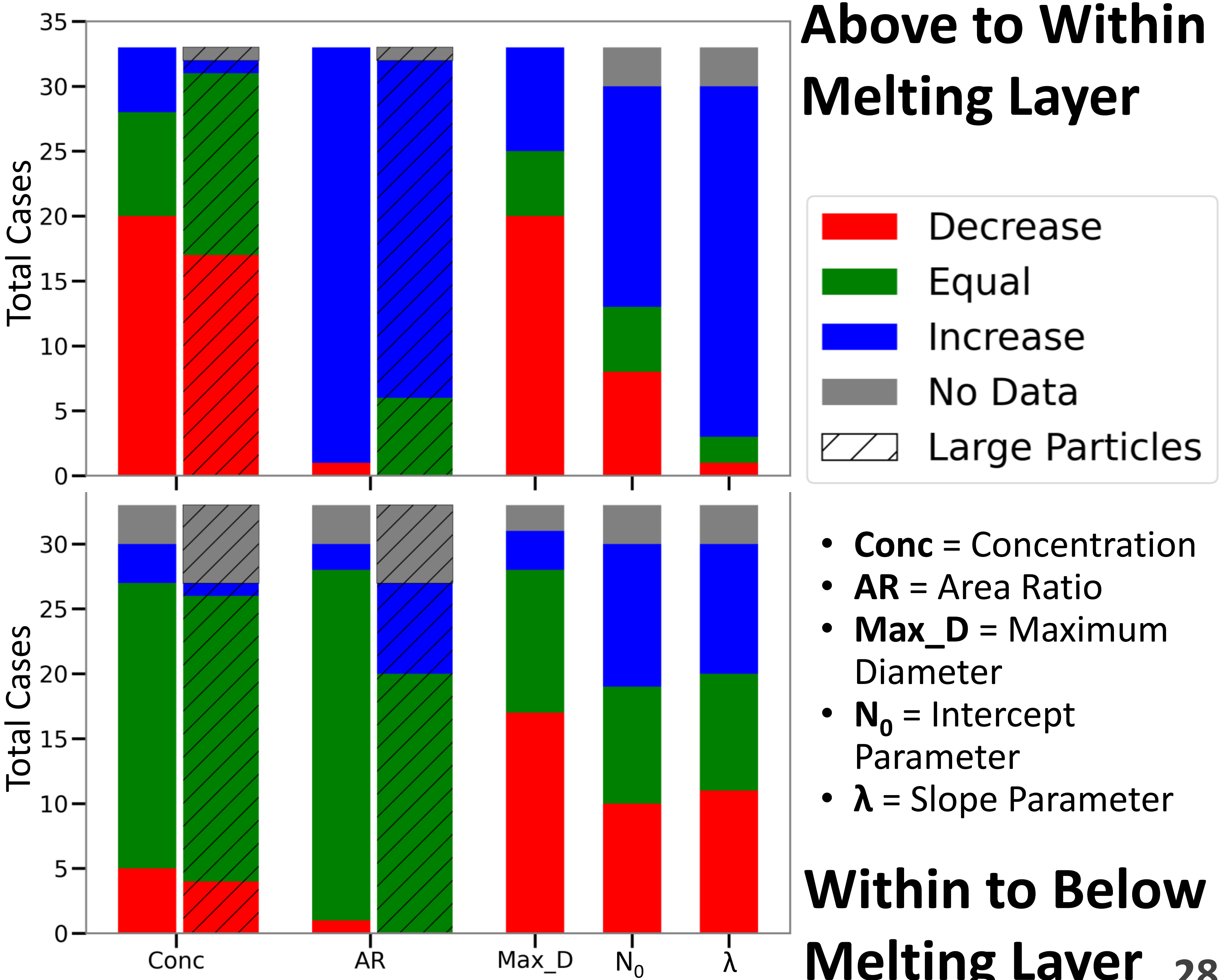

- **Conc** = Concentration
- **AR** = Area Ratio
- **Max_D** = Maximum Diameter
- $\mathbf{N_0}$ = Intercept Parameter
- **λ** = Slope Parameter

Within to Below Melting Layer

Conclusions

- An increase in area ratio over a depth indicates melting is occurring.
- Area ratio begins to increase below 0 °C ice-bulb isotherm.
  - Confirms Heymsfield et al. (2021).
- Concentration of both small and large hydrometeors decreases.
- Few cases have enhanced aggregation
- Only 2/33 cases have a quasi-isothermal layer

Summary Table

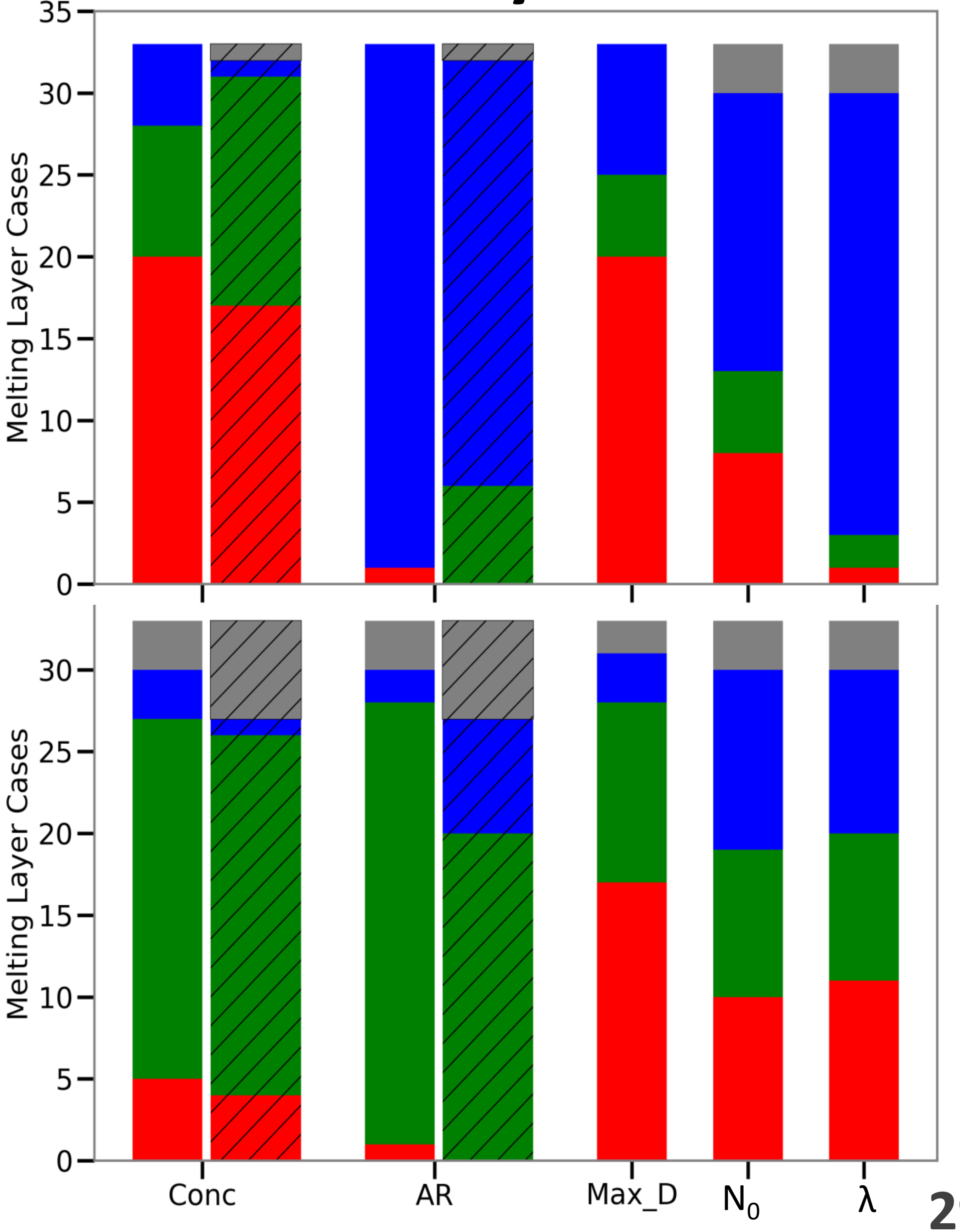

Future Work

- How is the lapse rate impacted?
- How do radar reflectivity changes in the melting layer compare to the observed particle spectrum changes?
  - How does this relate to the bright band?
- What happens to hydrometeors smaller than 500 µm?
  - Newer probes with larger sample volume than 2D-S but higher resolution than HVPS3?

Acknowledgements

- **Committee Members**
  - Dr. David Delene, UND
  - Dr. Michael Poellot, UND
  - Dr. Andrew Heysmfield, NCAR
- **UND Atmospheric Sciences Department**
  - Faculty Members
  - Students
- **Friends** and **Colleagues**
- **Family**

References

Delene, D. J., 2011: Airborne data processing and analysis software package. *Earth Sci Inform*, **4**, 29–44, https://doi.org/10.1007/s12145-010-0061-4.

Fabry, F., and I. Zawadzki, 1995: Long-Term Radar Observations of the Melting Layer of Precipitation and Their Interpretation. *Journal of the Atmospheric Sciences*, **52**, 838–851, https://doi.org/10.1175/1520-0469(1995)052<0838:LTROOT>2.0.CO;2.

Gorgucci, E., L. Baldini, and V. Chandrasekar, 2006: What Is the Shape of a Raindrop? An Answer from Radar Measurements. *Journal of the Atmospheric Sciences*, **63**, 3033–3044, https://doi.org/10.1175/JAS3781.1.

Heymsfield, A. J., and J. L. Parrish, 1978: A Computational Technique for Increasing the Effective Sampling Volume of the PMS Two-Dimensional Particle Size Spectrometer. *Journal of Applied Meteorology and Climatology*, **17**, 1566–1572, https://doi.org/10.1175/1520-0450(1978)017<1566:ACTFIT>2.0.CO;2.

——, ——, M. R. Poellot, and N. Wood, 2015: Observations of Ice Microphysics through the Melting Layer. *Journal of the Atmospheric Sciences*, **72**, 2902–2928, https://doi.org/10.1175/JAS-D-14-0363.1.

——, ——, A. Theis, and C. Schmitt, 2021: Survival of Snow in the Melting Layer: Relative Humidity Influence. *Journal of the Atmospheric Sciences*, https://doi.org/10.1175/JAS-D-20-0353.1.

Igel, A. L., and S. C. van den Heever, 2014: The role of latent heating in warm frontogenesis: The Role of Latent Heating in Warm Frontogenesis. *Q.J.R. Meteorol. Soc.*, **140**, 139–150, https://doi.org/10.1002/qj.2118.

Iversen, E. C., G. Thompson, and B. E. Nygaard, 2021: Improvements to melting snow behavior in a bulk microphysics scheme. *Atmospheric Research*, **253**, 105471, https://doi.org/10.1016/j.atmosres.2021.105471.

Kain, J. S., S. M. Goss, and M. E. Baldwin, 2000: The Melting Effect as a Factor in Precipitation-Type Forecasting. *Weather and Forecasting*, **15**, 700–714, https://doi.org/10.1175/1520-0434(2000)015<0700:TMEAAF>2.0.CO;2.

Marshall, J. S., and W. M. K. Palmer, 1948: THE DISTRIBUTION OF RAINDROPS WITH SIZE. *Journal of the Atmospheric Sciences*, **5**, 165–166, https://doi.org/10.1175/1520-0469(1948)005<0165:TDORWS>2.0.CO;2.

Mitra, S. K., O. Vohl, M. Ahr, and H. R. Pruppacher, 1990: A Wind Tunnel and Theoretical Study of the Melting Behavior of Atmospheric Ice Particles. IV: Experiment and Theory for Snow Flakes. *Journal of the Atmospheric Sciences*, **47**, 584–591, https://doi.org/10.1175/1520-0469(1990)047<0584:AWTATS>2.0.CO;2.

Stewart, R. E., J. D. Marwitz, J. C. Pace, and R. E. Carbone, 1984: Characteristics through the Melting Layer of Stratiform Clouds. *Journal of the Atmospheric Sciences*, **41**, 3227–3237, https://doi.org/10.1175/1520-0469(1984)041<3227:CTTMLO>2.0.CO;2.

Willis, P. T., and A. J. Heymsfield, 1989: Structure of the Melting Layer in Mesoscale Convective System Stratiform Precipitation. *Journal of the Atmospheric Sciences*, **46**, 2008–2025, https://doi.org/10.1175/1520-0469(1989)046<2008:SOTMLI>2.0.CO;2.

Psychrometric formula - Glossary of Meteorology. https://glossary.ametsoc.org/wiki/Psychrometric_formula (Accessed May 2, 2022).


QUESTIONS?

Ice-bulb Comparison

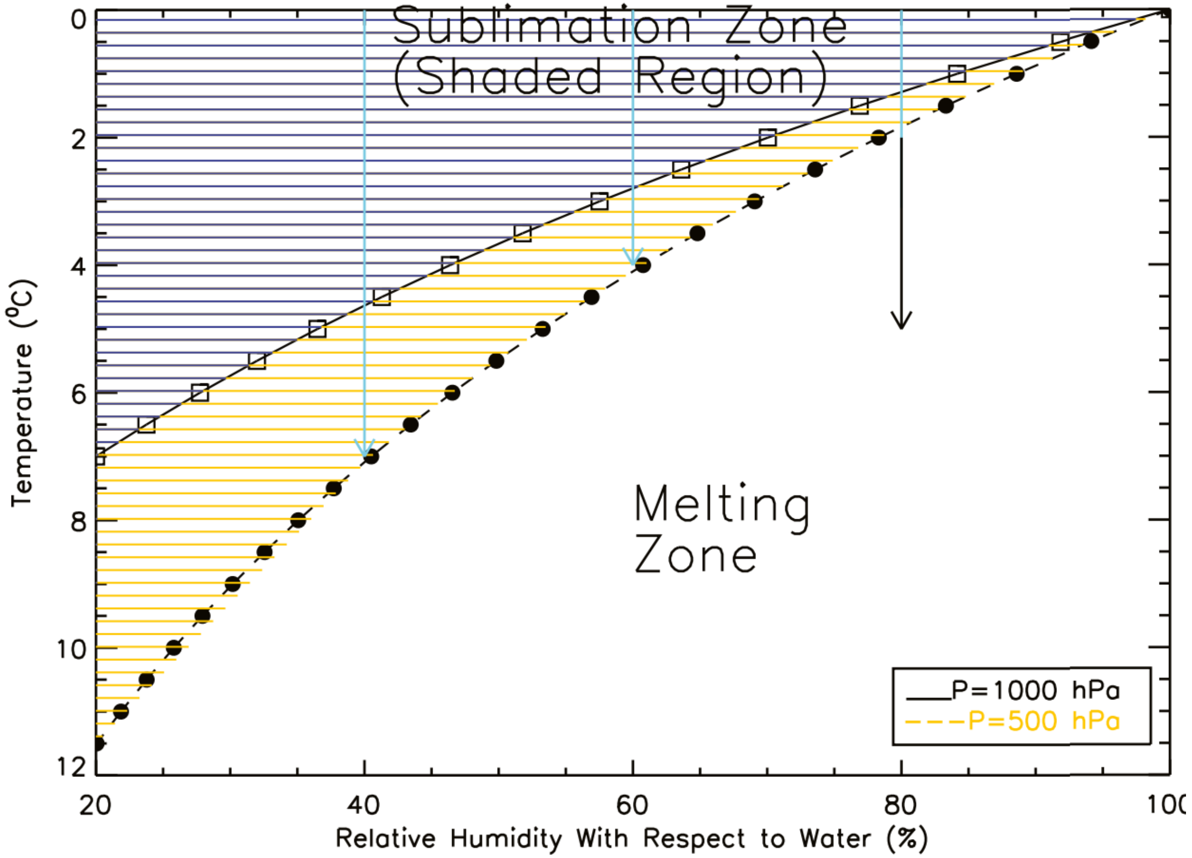

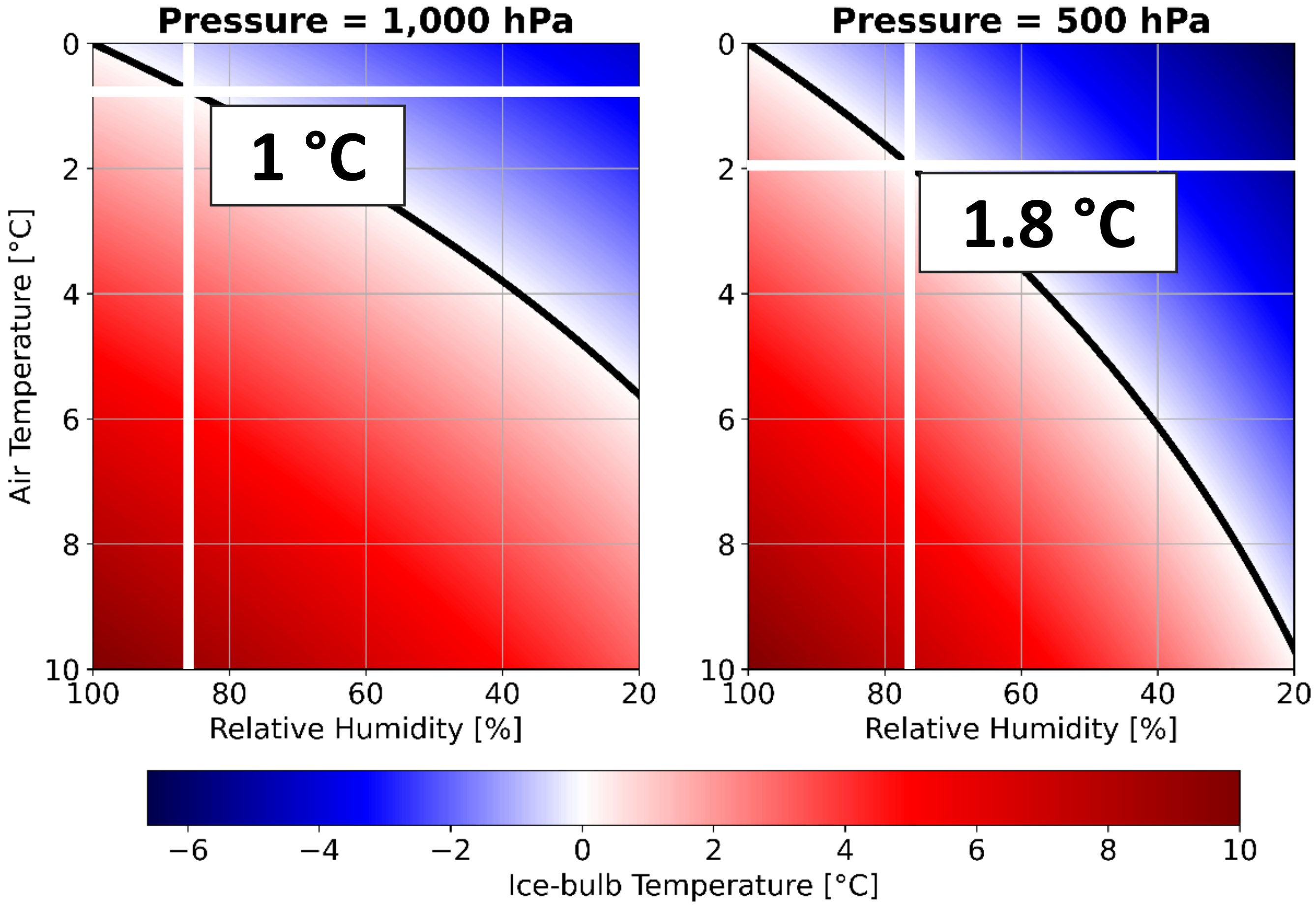

Ice-bulb Temperature

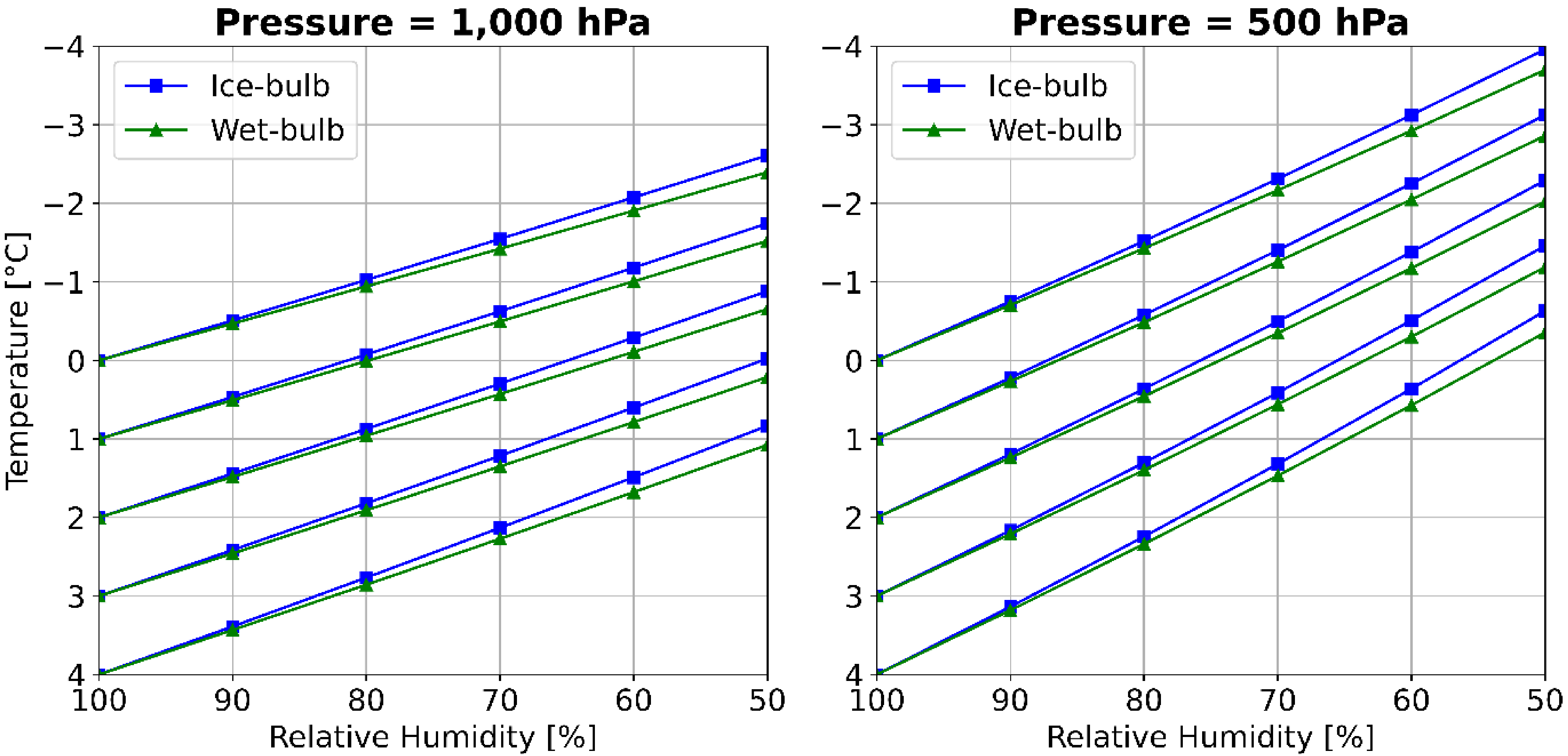

Ice-bulb Derivation

$$e_s(T) = e_0 \exp\left[\frac{l_v}{R_v}\left(\frac{1}{T_0} - \frac{1}{T}\right)\right] \qquad e(T_d) = e_0 \exp\left[\frac{l_v}{R_v}\left(\frac{1}{T_0} - \frac{1}{T_d}\right)\right]$$

$$e_{IB}(T_{IB}) = e_0 \exp\left[\frac{l_v}{R_v}\left(\frac{1}{T_0} - \frac{1}{T_{IB}}\right)\right]$$

$$e = e_{IB}(T_{IB}) - 5.82 \times 10^{-4} \, (1 + 0.00115 \, \mathrm{T_w}) \, \mathrm{p} \, (\mathrm{T} - \mathrm{T_w})$$

2D-S vs. HVPS3

- Zero counts in 2D-S

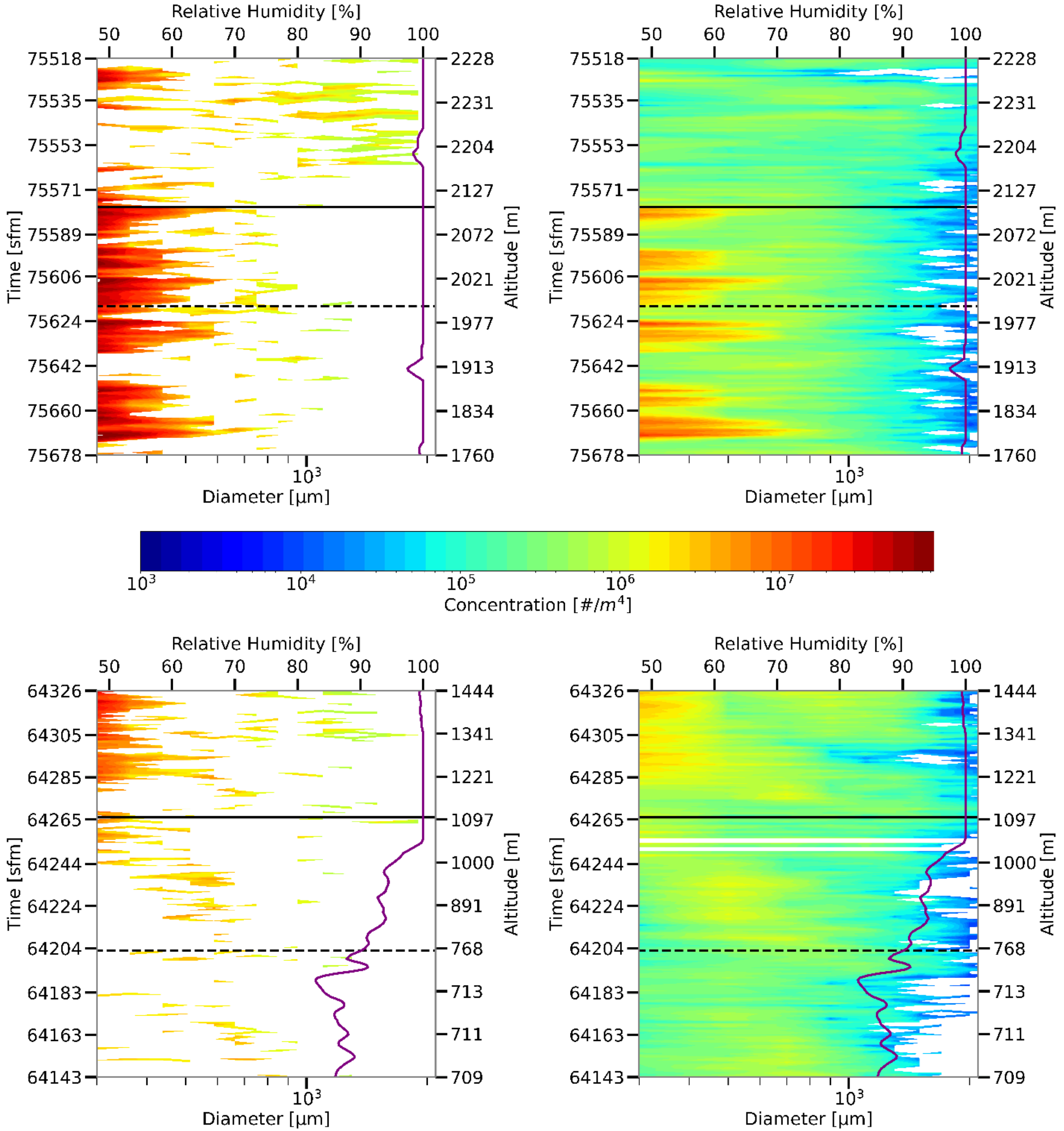

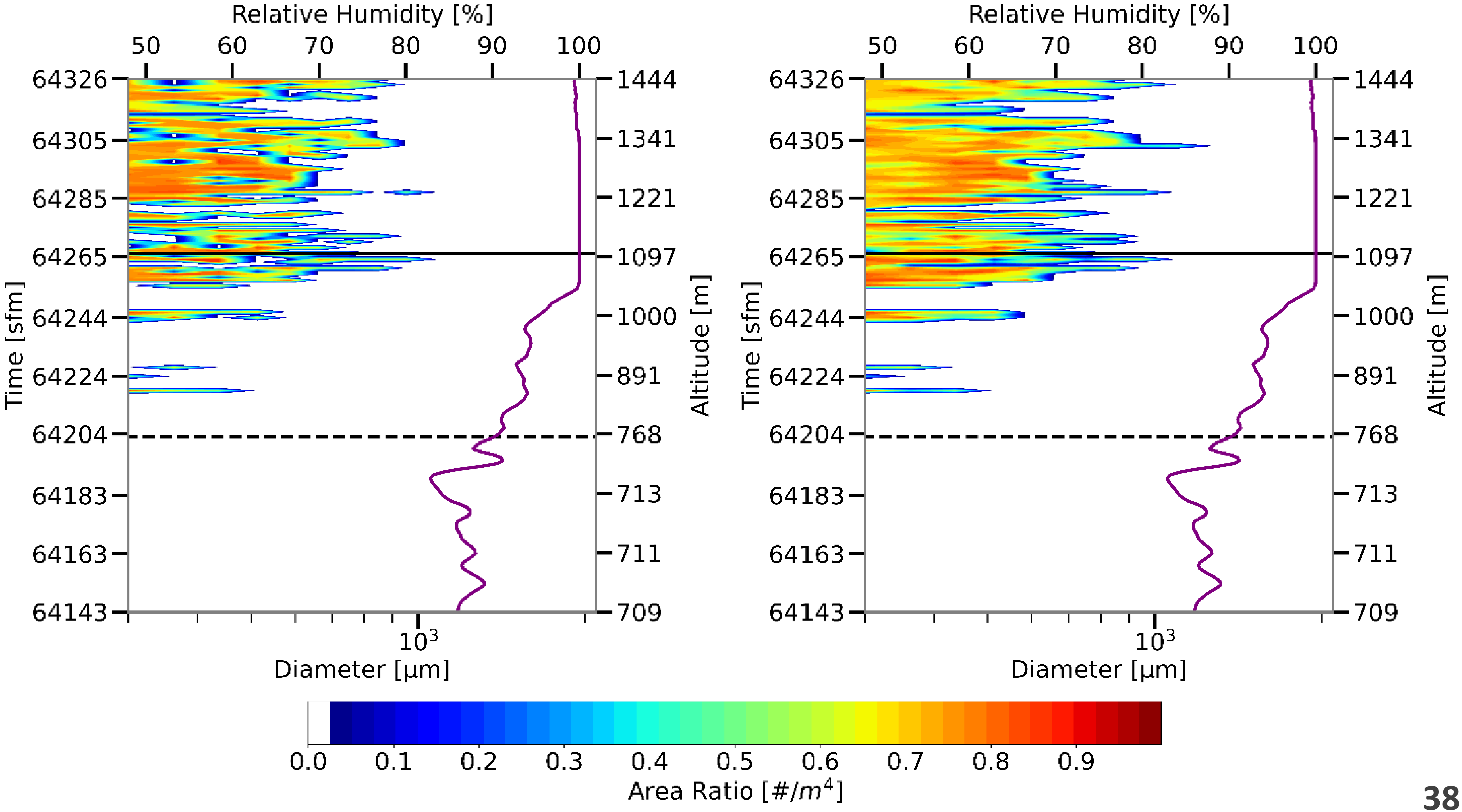

Relative Humidity [%]
50
60
70
80
90
100
64326
64305
64285
64265
64244
64224
64204
64183
64163
64143
Time [sfm]
1444
1341
1221
1097
1000
891
768
713
711
709
Altitude [m]
10^3
Diameter [µm]
Relative Humidity [%]
Time [sfm]
Altitude [m]
Diameter [µm]
0.0
0.1
0.2
0.3
0.4
0.5
0.6
0.7
0.8
0.9
Area Ratio [$\#/m^4$]

Pixels Necessary for Area Ratio Analysis

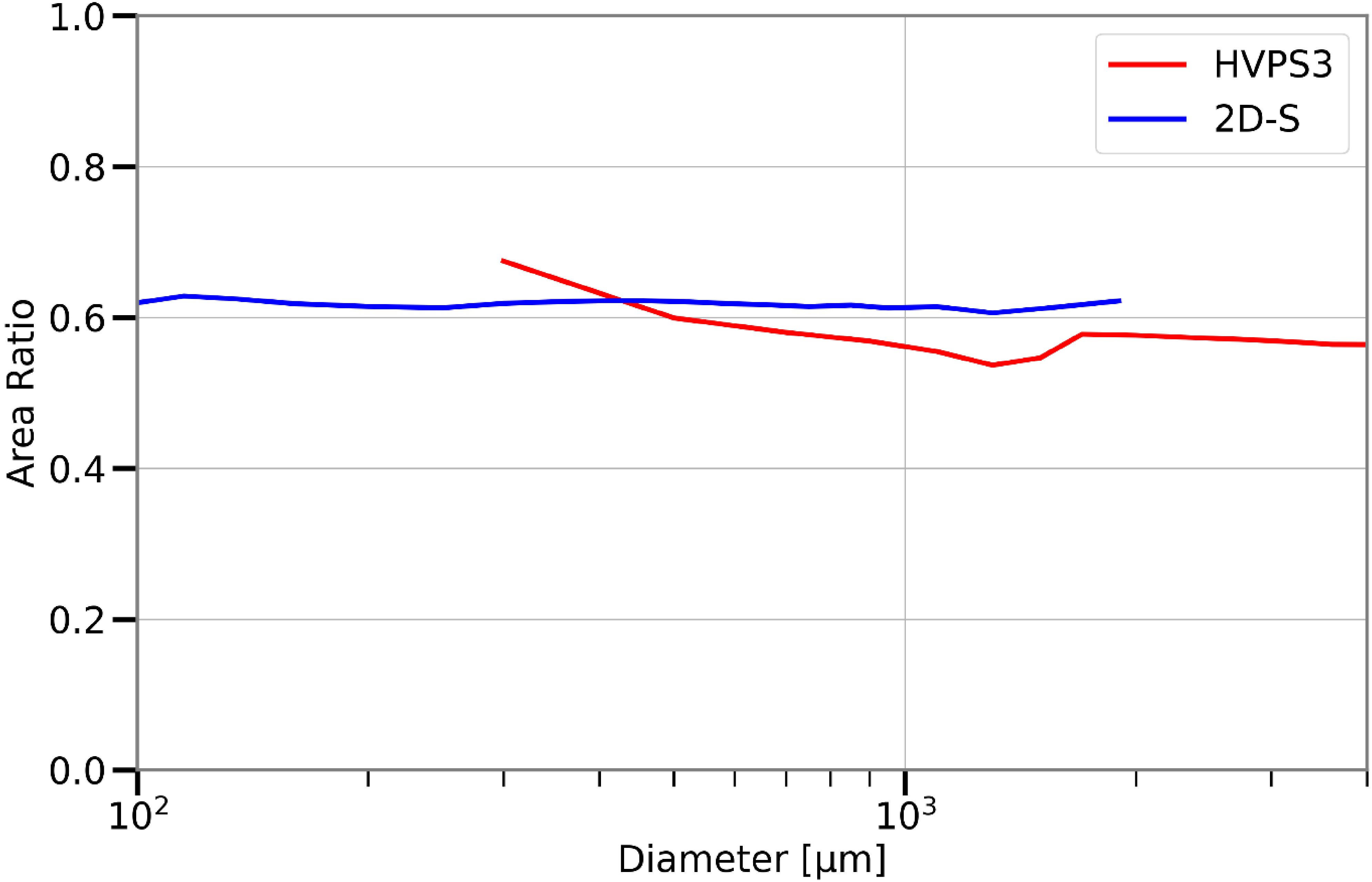

Melting Layer Cases

	Low (≤ 90%) RH	High (> 90%) RH	Saturated	Total
Spiral	4	8	6	18
Ramp	5	9	1	15
Total	**9**	**17**	**7**	**33**

Liquid Water Content: 12 November 2015

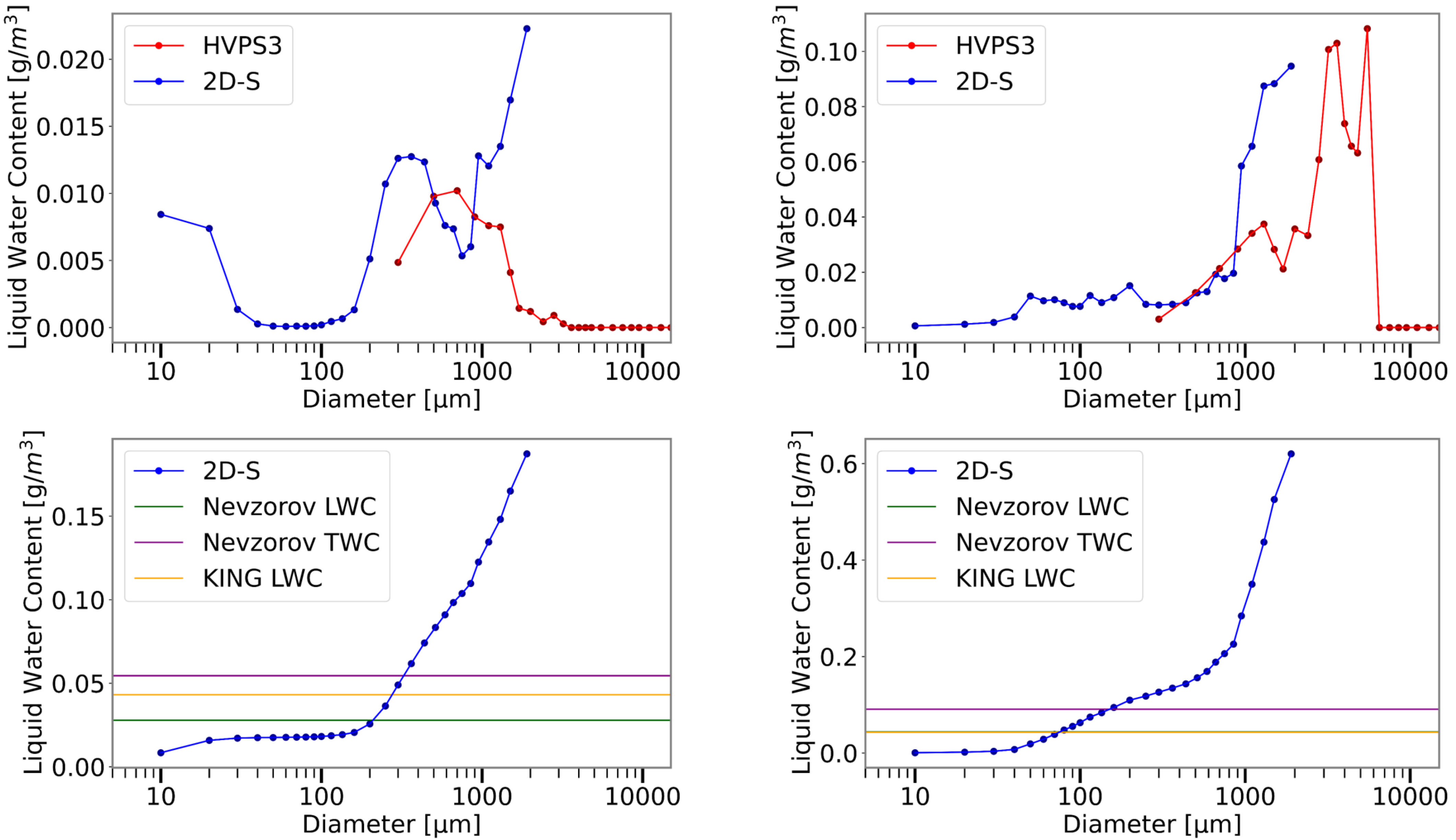

Liquid Water Content: 12 November 2015

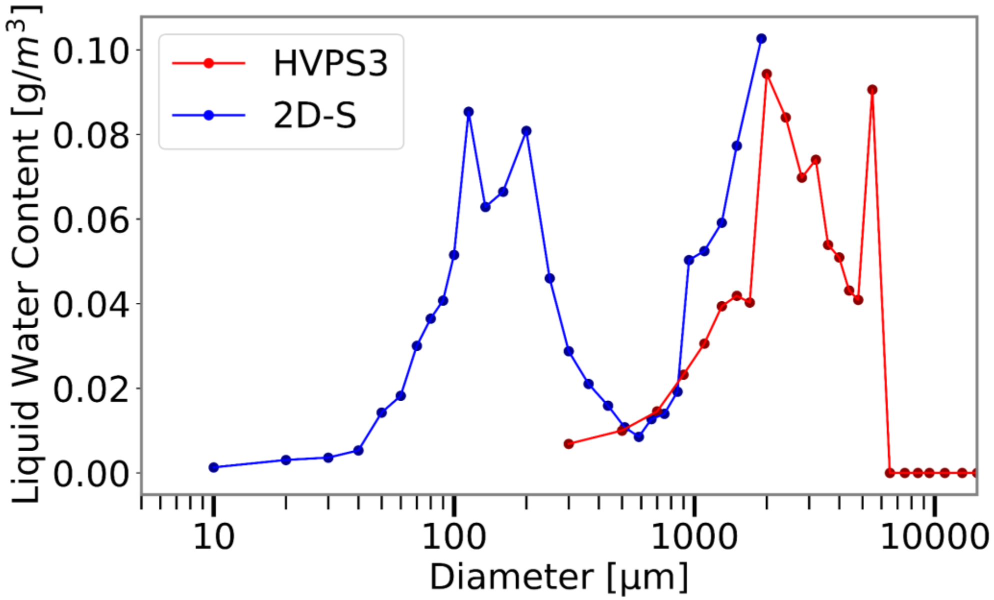

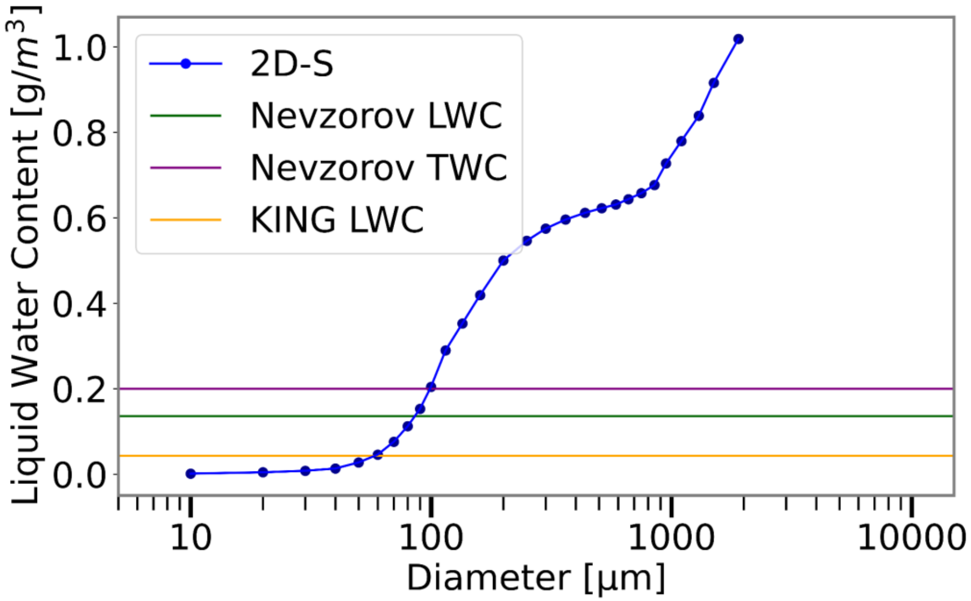

One Melting Layer Sampled Twice During MC3E

- Melting layer top around 3,750 m
- Depths of 133 m (descent) and 123 m (ascent)
- RH of 83% and 79%
- 0 °C isotherm is 235 m higher during the ascent

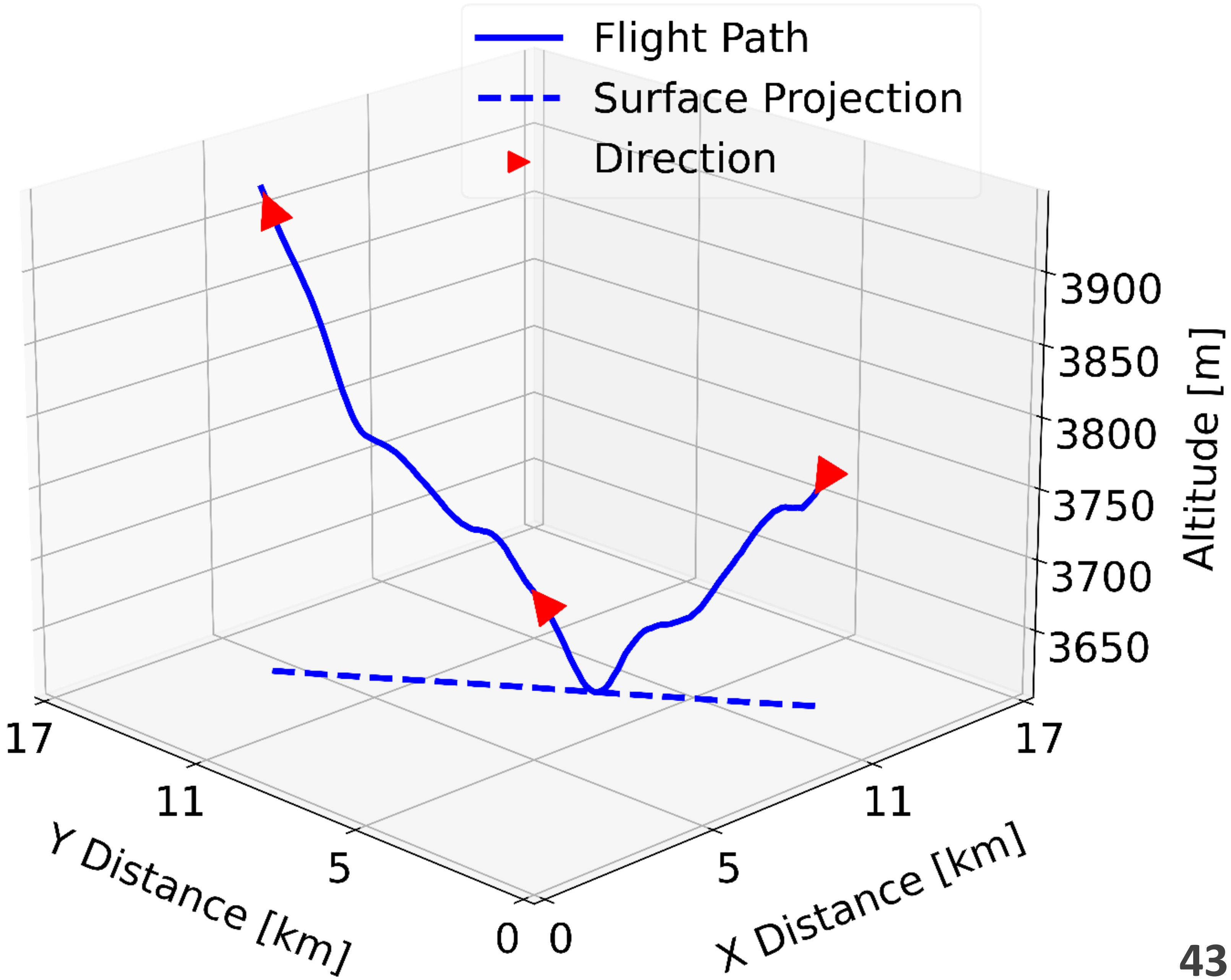

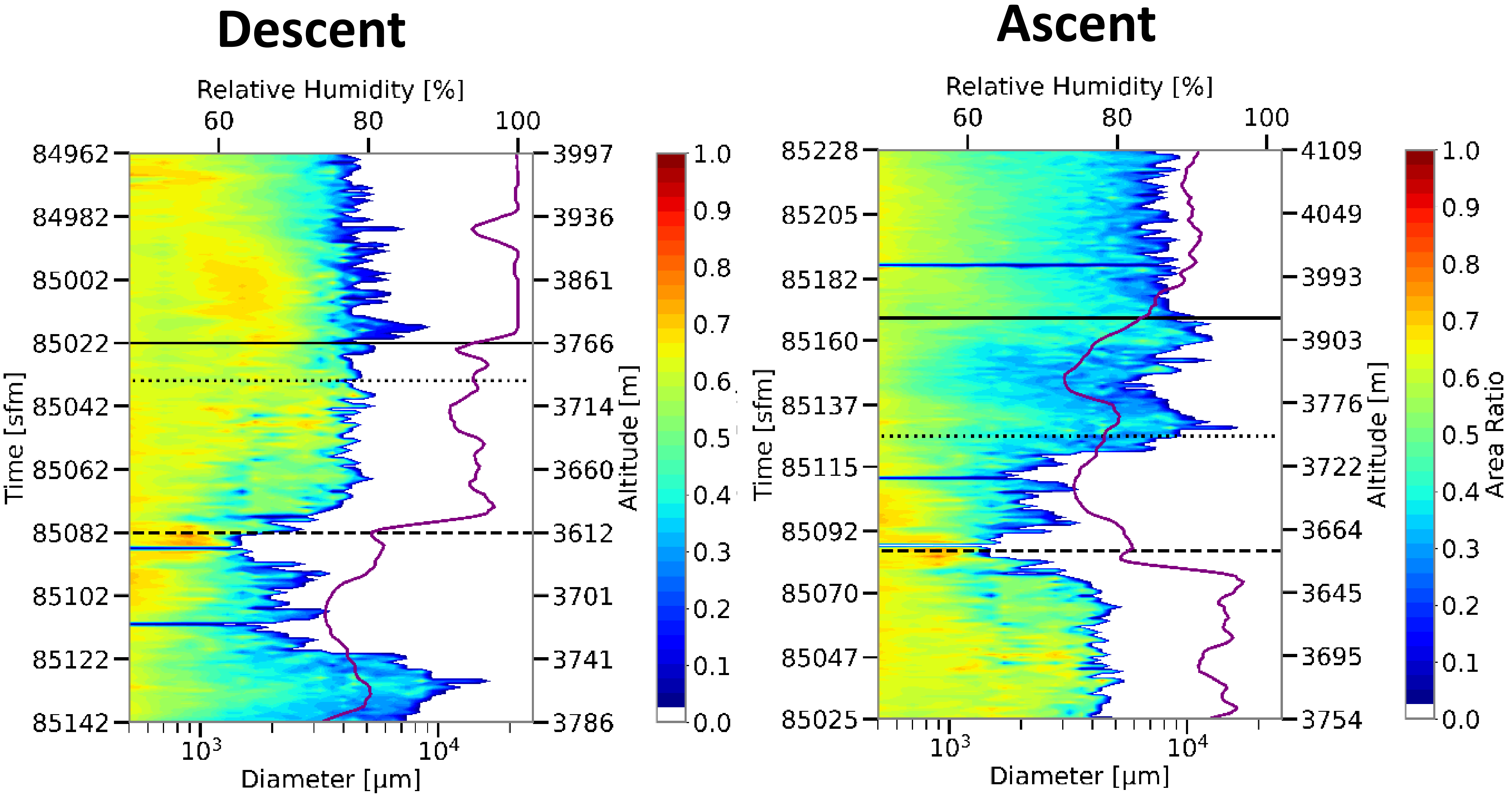
Descent
Ascent
Relative Humidity [%]
60
80
100
Time [sfm]
84962
84982
85002
85022
85042
85062
85082
85102
85122
85142
Altitude [m]
3997
3936
3861
3766
3714
3660
3612
3701
3741
3786
Diameter [µm]
10^3
10^4
85228
85205
85182
85160
85137
85115
85092
85070
85047
85025
4109
4049
3993
3903
3776
3722
3664
3645
3695
3754
Area Ratio
1.0
0.9
0.8
0.7
0.6
0.5
0.4
0.3
0.2
0.1
0.0

IPHEX_Spi-Asc_100RH

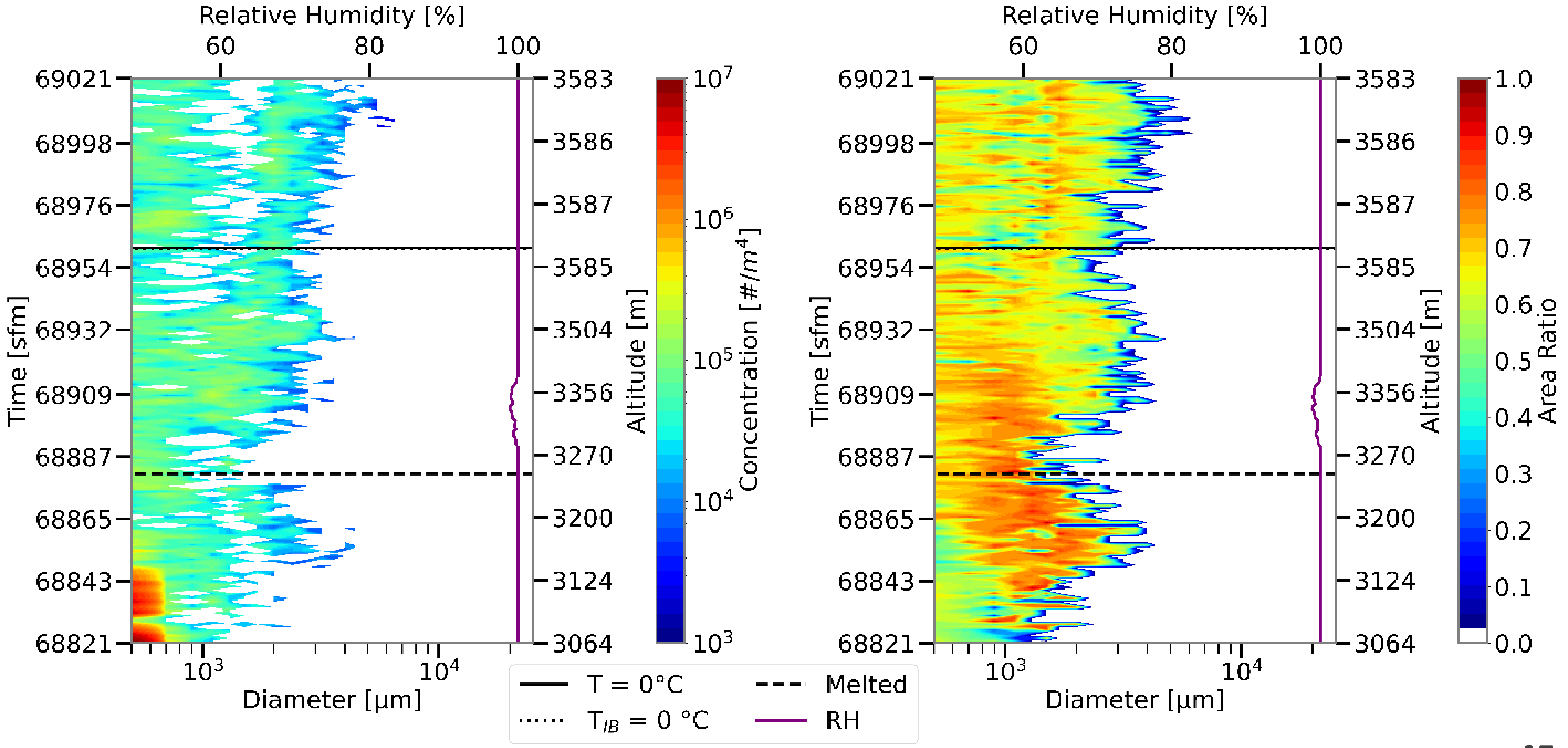

IPHEX_Ram-Asc_92RH

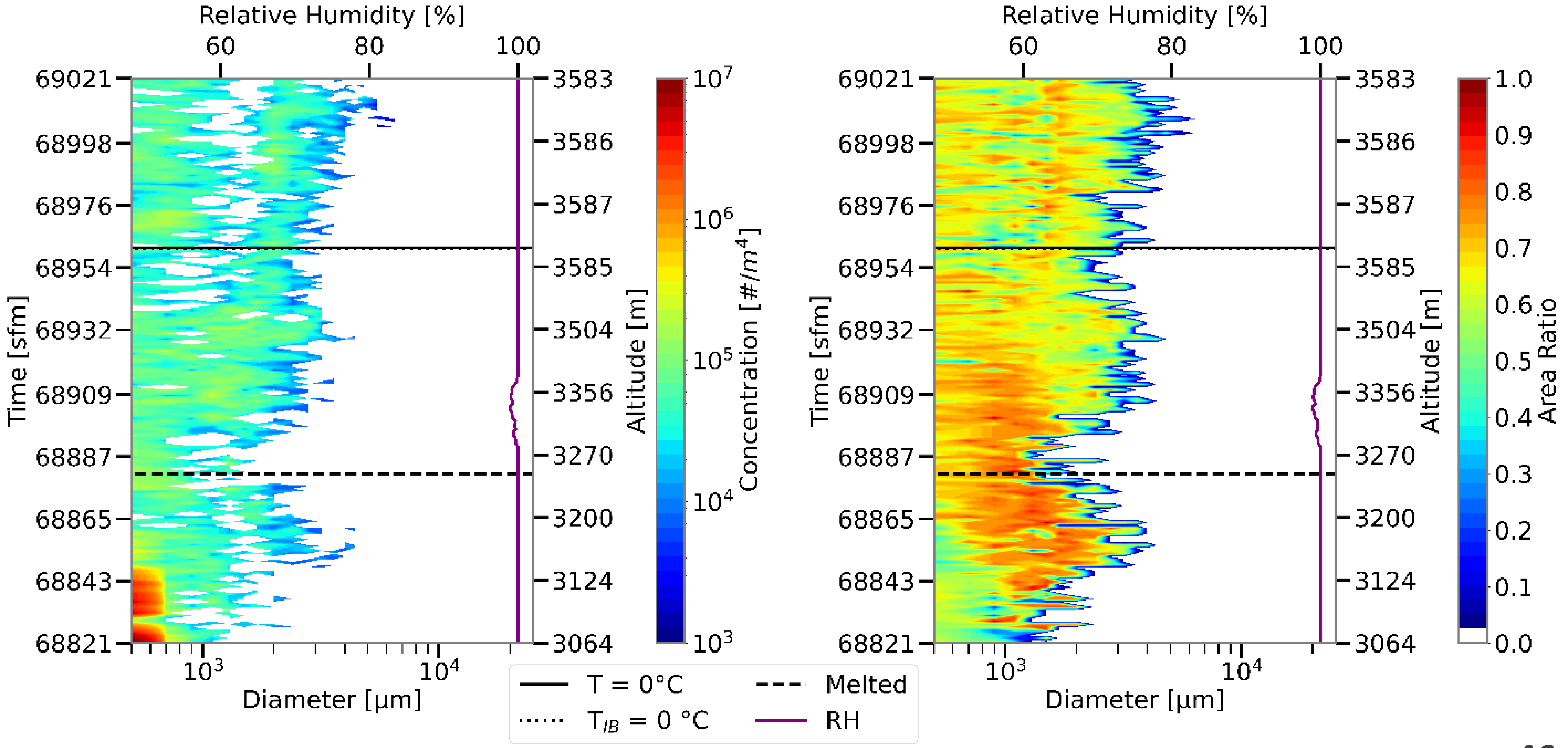

OLYMPEX_Spi-Des_100RHa

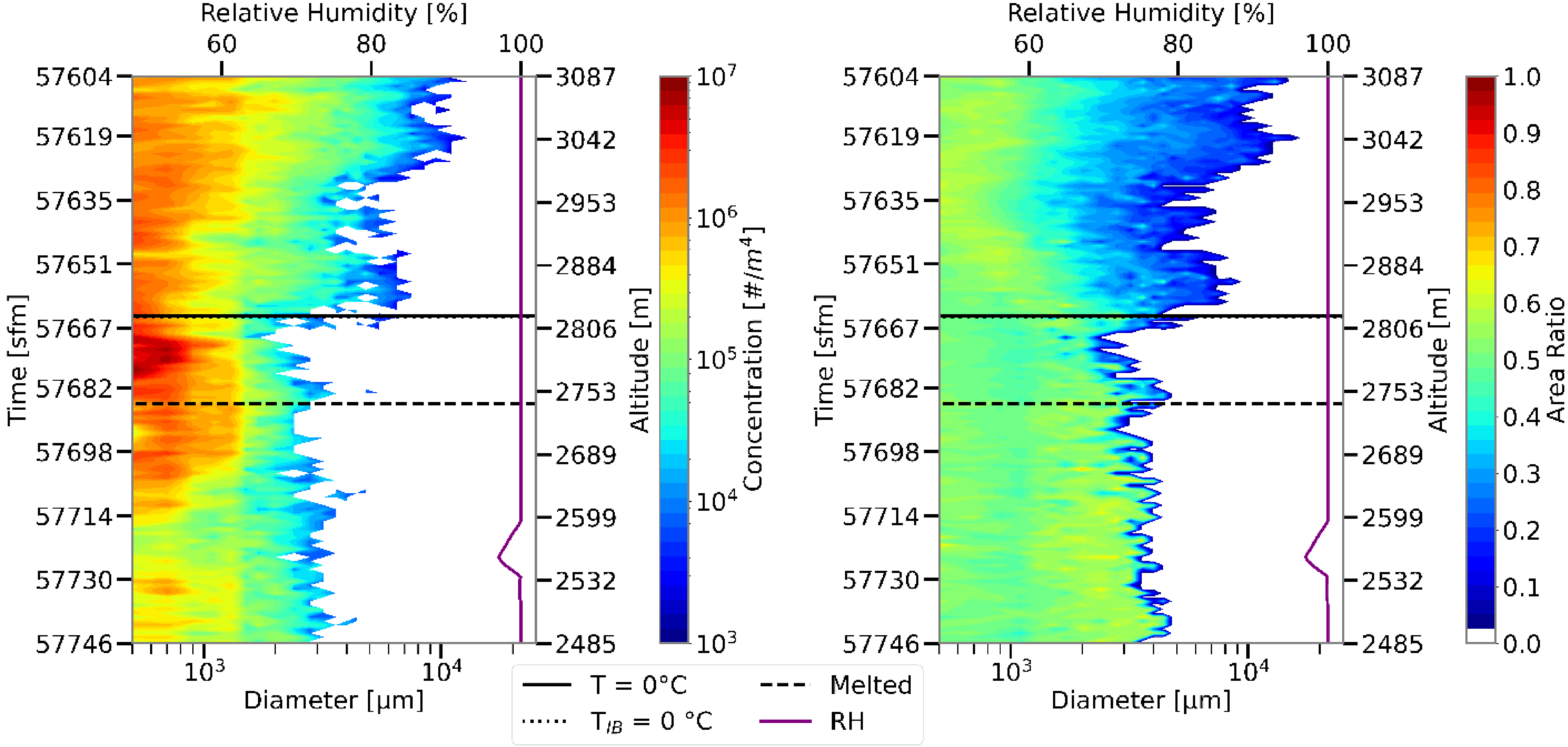

GCPEX_Ram-Des_71RH

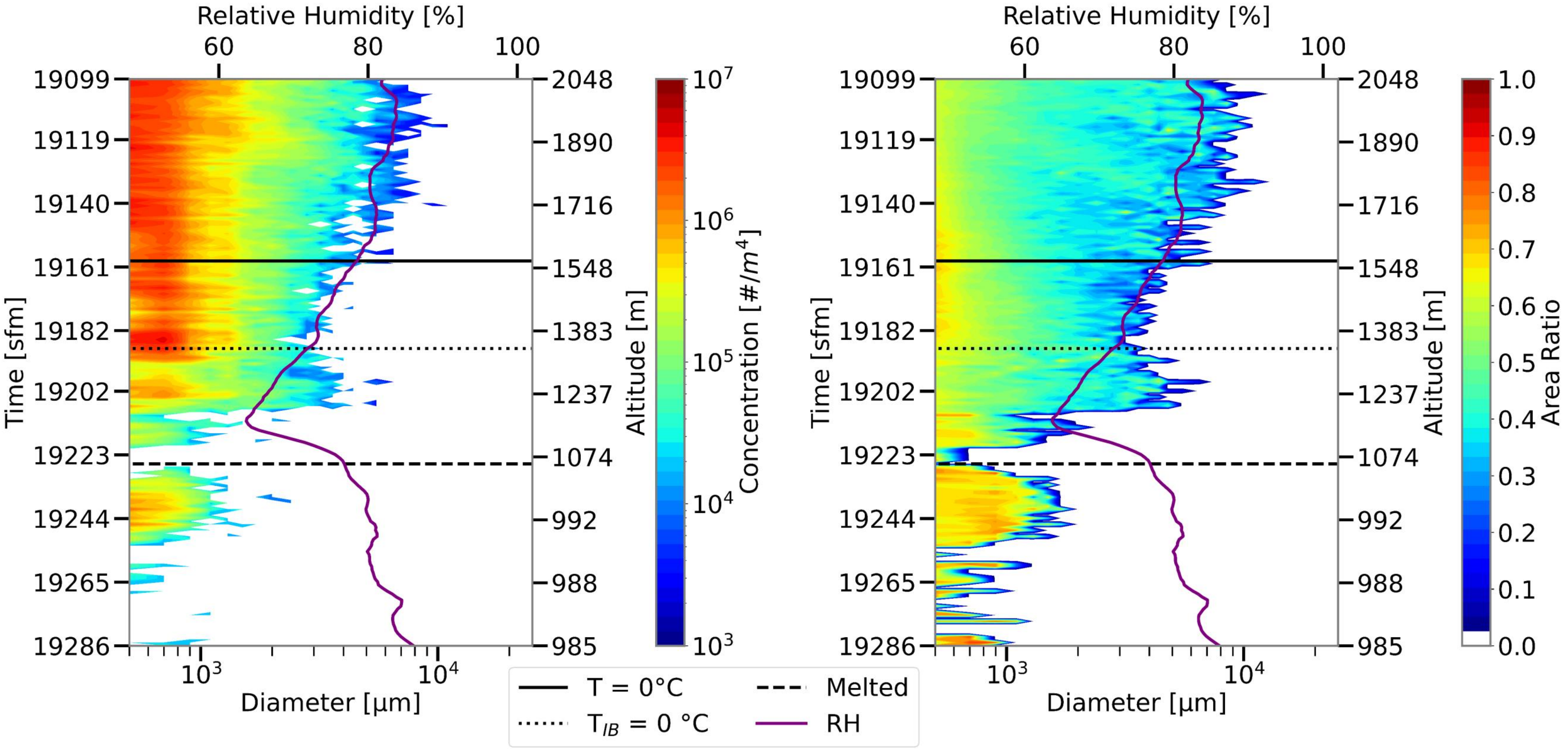

IPHEX_Ram-Asc-92RH